β-Phosphorus Hyperfine Coupling Constant in Nitroxides: 5. Solvent Effect"

Journal Name

ARTICLE

β-Phosphorus Hyperfine Coupling Constant in Nitroxides: 5. Solvent Effect

Gérard Audran,[*a] Lionel Bosco,[a] Paul Brémond,[a] Teddy Butscher,[a] Jean-Michel Franconi,[b] Kuanysh Kabitaev, Sylvain R. A. Marque,[a,c]* Philippe Mellet,[b,d] Elodie Parzy,[b] Maurice Santelli,[a] Eric Thiaudière[b] and Stephane Viel[a]

Recently, we publihed the titration of water in organic solvents and conversely using this family of nitroxides (*Org. Biomol. Chem.* **2015** ASAP). In this article, we show that the $a_{\beta,P}$ of persistent cyclic β-phosphorylated nitroxides decrease with the normalized polarity Reichardt's constant E_T^N. Koppel-Palm and Kalmet-Abboud-Taft relationships were applied to get deeper insight into the effects influencing a_N and $a_{\beta,P}$: polarity/polarizability, Hydrogen Bond Donor property, and *structuredness* of the cybotactic region.

Introduction

Persistent nitroxides[1,2] find applications in Biology as pH-probes[3] or spin probes,[4] in Spectroscopy as agents for Dynamic Nuclear Polarization enhanced Nuclear Magnetic Resonance (DNP-NMR),[5-7] or in Material Sciences for organic magnetic materials.[8] Their spectroscopic properties, which are represented by the nitrogen hyperfine coupling constant a_N, are the cornerstone of most of these applications. Several investigations of the solvent effects in the cybotactic region are available in the literature.[9-12] They showed that a_N increased when increasing the normalized solvent-polarity Reichardt's constant E_T^N,[13,14] as exemplified with **1•** (Figure 1). Some studies showed that the hyperfine coupling constants of hydrogen and of fluorine atoms at the position β, $a_{H\beta}$[10] and $a_{F\beta}$,[11] are weakly sensitive to the polarity of the solvent as well as to the temperature. However, in 1976, Il'Yasov and coll.[12] showed a dramatic change $\Delta a_{\beta,P}$ in the phosphorus hyperfine coupling constants $a_{\beta,P}$ with $E_{T(30)}$ (a $\Delta a_{\beta,P}$ of ca. 20 G between *n*-hexane and water) with nitroxide **2•** (Figure 1).[#] A few years laters, Janzen and coll.[15] reported a similar effect with β-phosphorylated cyclic nitroxides (only 3 solvents were

investigated). On the other hand, with the persistent[16] *N*-(2-methylpropyl)-*N*-(1-diethylphosphono-2,2-dimethylpropyl)-*N*-oxyl radical (**2'•** in Figure 1) we[17] recently showed that $a_{\beta,P}$ was weakly sensitive to E_T^N, with a lot of outliers for alcoholic solvents and water. We also reported[18] a non linear variation in $a_{P\beta}$ with E_T^N for the stable nitroxide **2"•**. Moreover, with **2''•** and **5c,t•**, we highlighted the potential of theses nitroxides to probe the presence of water in organic solvents and conversely.[18,19] It is well known that β-phosphorylated pyrrolidin-based nitroxides are persistent[16,20] and that the changes in conformation of the 5-membered ring can strikingly modify the values of $a_{\beta,P}$, as given by the Heller-McConnell relationship[21] (eq. 1), by modifying the dihedral angle θ between the C—P bond and the p-shape orbital describing the odd electron localized (Figure 2) on the nitrogen atom of the nitroxyl moiety (where ρ_N^π is the electron density on the nitrogen atom of the nitroxyl moiety and proportional to the a_N value, $B_0^{\S}$ is the transfer of the spin density through the spin polarization process and $B_1^{\dagger}$ is the transfer of spin density through the hyperconjugation process):

$$a_{\beta,P} = B_0 \cdot \rho_N^\pi + B_1 \cdot \rho_N^\pi \cdot \cos^2\theta \qquad (1)$$

Surprisingly, β-phosphorylated nitroxides carrying a substituted methylene group at position β (Figure 1) have been only little investigated[15,22,23] and mainly by spin-trapping.[24-27] Thus, several nitroxides carrying various groups at position β were prepared (Figure 1), aiming both to vary the steric hindrance and to investigate the effect of stereogenic centres at the α positions of the nitroxyl moiety. A few investigations of the effect of a substituent at position 3 or 4 as well as of the effect of the configuration at positions 2, 3, and 4 for 2,5,5-trimethyl-2-diethoxyphosphonyl-pyrrolidin-*N*-

[a.] *Aix-Marseille Université, CNRS-UMR 7273, ICR, case 541, Avenue Escadrille Normandie-Niemen, 13397 Marseille Cedex 20 France.*
[b.] *CRMSB, CNRS-UMR-5536, Université Victor Segalen Bordeaux 2, 146 rue Léo Saignat, Case 93, 33076 Bordeaux cedex, France*
[c.] *N. N. Vorozhtsov Novosibirsk Institute of Organic Chemistry SB RAS, Pr. Lavrentjeva 9, 630090 Novosibirsk, Russia.*
[d.] *INSERM, 146 rue Léo Saignat, Case 93, 33076 Bordeaux cedex, France*
* *to whom the correspondence should be sent:* paul.brémond@univ-amu.fr, sylvain.marque@univ-amu.fr, g.audran@univ-amu.fr
Electronic Supplementary Information (ESI) available: Table 1SI for the solvent parameters. Figure 1SI for plots a_N vs μ, a_N vs ε_r, $a_{\beta,P}$ vs μ and $a_{\beta,P}$ vs ε_r. Figure 2SI for plots a_N against *c*, V_X (Å), V_M (Å), α and π* and $a_{\beta,P}$ against *c*, V_X (Å), V_M (Å), α and π* (right). Preparation of **4•** and **5•**. See DOI: 10.1039/x0xx00000x

oxyl radicals on a_N and $a_{\beta,P}$ have been reported.[28,29] Indeed, an extensive investigation on the solvent effect in β-phosphorylated is timely due to their various applications: *i)* as products issued from the spin-trapping of radicals by β-phosphorylated nitroxides taking into account that only a little is known on the solvent effect on spin-adducts and often the trapped radicals are rather basics such as Me•, HO•, HOO• ….; *ii)* as component of alkoxyamines which are currently used as initiator/controller in Nitroxide Mediated Polymerization.[30] The most efficients are often based on β-phosphorylated nitroxyl moiety;[31] *iii)* as new spin-label for Site Directed Spin Labeling (SDSL) for which changes in hcc might provide information on the folding-unfolding process,[32] and *iv)* as spin probe to investigate non-radical enzymatic activity by Overhauser-enhanced Magnetic Resonance Imaging (OMRI) and EPR.[33]

Results

Preparation of nitroxides 3•-7t•.

Nitroxides **3•**[34] and **7t•**[35] were prepared as reported in the literature. Aziridine **3** was prepared as recently reported from commercially available 6-methylhex-5-en-2-one **1** (Scheme 1).[35] Aziridine **3** was obtained as two diastereoisomers *cis* (**3c**) and *trans* (**3t**), which were separated by column chromatography on silica gel. Their relative configuration was determined by NMR and X-ray studies (*vide infra*).

The nucleophilic addition of acetic acid onto **3c,t** afforded adducts **4c,t** in 62-70%. They were subsequently oxidized by *m*-CPBA (90-94% yield) into nitroxides **4c•** and **4t•** (Scheme 2). Then, **4c•,t•** were treated by potassium carbonate in MeOH to afford **10c•,t•** (80-90% yield), which were then esterified with pivaloyl chloride (82% yield) to afford **5c•** and **5t•**, respectively (Scheme 3).
The nucleophilic addition of sodium azide onto **3c** and **3t** afforded **6c** and **6t**, respectively, which were subsequently oxidized into nitroxides **6c•** and **6t•** (Scheme 4).
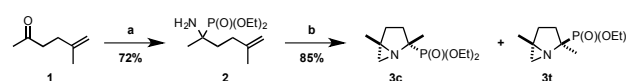
Scheme 1. Preparation of the aziridine key-intermediate **3**. Reagents and conditions: (a) NH₃, HP(O)(OEt)₂, 24 h, r.t.; (b) I₂, NaHCO₃, 1,2-dichloroethane, H₂O, 2 h, reflux.
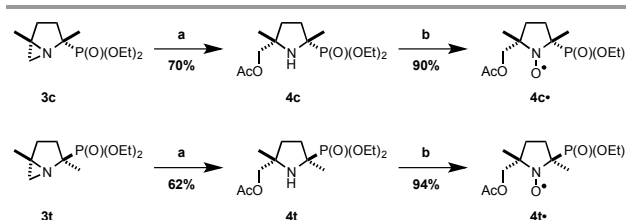
Scheme 2. Synthesis of **4c,t•**. Reagents and conditions: (a) AcOH, 24 h, r.t; (b) *m*-CPBA, CH₂Cl₂, 2 – 4 h, r.t.
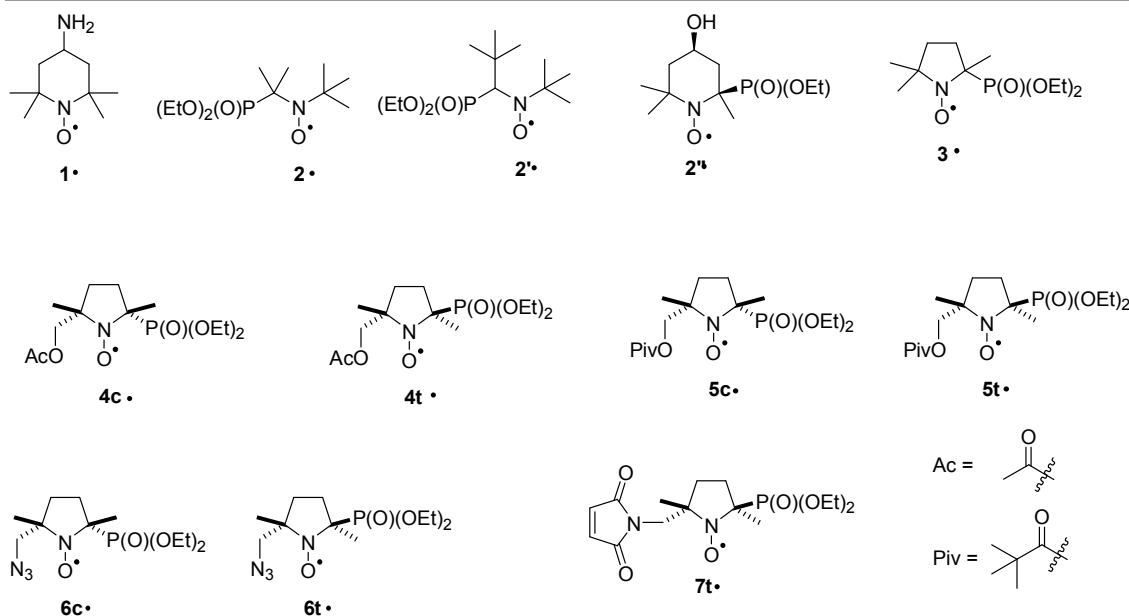
Figure 1. Nitroxides investigated: **c** for the *cis* isomer and **t** for the *trans* isomer.

Journal Name

ARTICLE
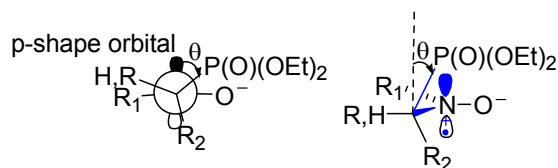
Figure 2. Hyperconjugation effect describing the origin of the coupling between the nuclear spin of the phosphorus atom and the p-shape orbital on the N atom of the nitroxyl moiety. Newman projection on the left, dihedral angle θ (in blue) on the Cram projection on the right.
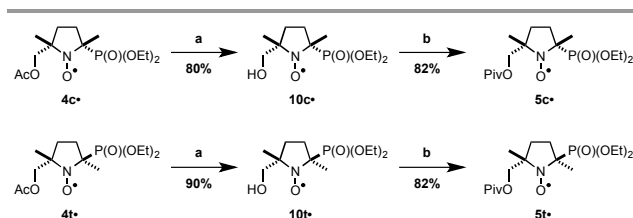
Scheme 3. Synthesis of **5c,t•**. Reagents and conditions: (a) K_2CO_3, MeOH, 24 h, r.t.; (b) PivCl, Et_3N, DMAP, CH_2Cl_2, 24 h, r.t.

Scheme 4. Synthesis of **6c,t•**. Reagents and conditions: (a) NaN_3, NH_4Cl, CH_3CN, 3 h, reflux; (b) *m*-CPBA, CH_2Cl_2, r.t., 1 h.

NMR, EPR and X-ray analyses.

Once aziridines **3c** and **3t** were separated, **6c** (minor diastereoisomer) and **6t** (major diastereoisomer) were prepared by a univocal route (Scheme 4). Their relative configuration was determined using NOESY experiments. The Overhauser effect was observed between the two methyl groups f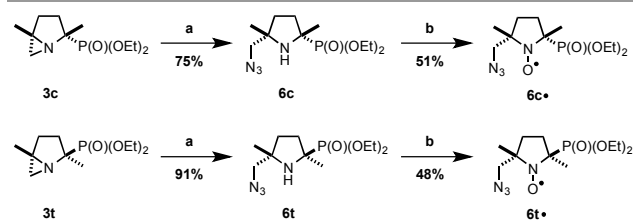or **6c** whereas it was not observed for **6t** (Figure 3).[‡] The relative configuration was definitely ascribed by the X-ray analysis of **10t•** (Figure 4),[£] which nicely confirmed the NOESY experiment, as **10t•** was also prepared through a univocal route from **3t** (Scheme 2-3). Consequently, the stereochemistry of each stereocenter in **4•** - **6•** (Figure 1) was ascertained from these two molecules.
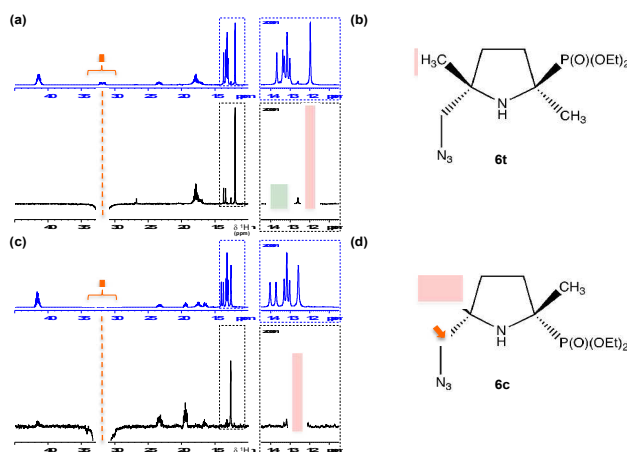
Figure 3. 500.13 MHz one-dimensional (1D) ^{1}H NMR and ^{1}H selective NOE NMR spectra (blue and black traces, respectively) recorded at 300 K in $CDCl_3$ solutions of (a) **6t** and (c) **6c**, the molecular structures of which are reported in (b) and (d), respectively. The orange arrows shown in (a) and (c) indicate the signals that were selectively irradiated in the 1D ^{1}H NOE NMR experiments and that correspond to the CH_2 protons (AB spin system) of the pendant CH_2N_3 moiety. Dotted zones in right side in (a) and (c) correspond to a zoom from the dotted zone on the main spectrum. The green and pink colored zones in (a) – (d) highlight the zones sensitive to the irradiation of the CH_2N_3 group.
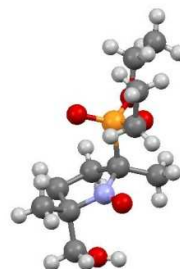
Figure 4. X-ray analysis of **10t•**.

Journal Name

ARTICLE

Table 1. Nitrogen and phosphorus hyperfine coupling constants a_N and $a_{P\beta}$,[a] respectively, in various solvents for nitroxides **1•-8•**.

	Solvent[b]	1•[c]	2•[d]		3•[e]		4c•		4t•		5c•		5t•		6c•		6t•		7t•	
		a_N	a_N	$a_{\beta,P}$	a_N	$a_{\beta,P}$	a_N	$a_{\beta,P}$	a_N	$a_{\beta,P}$	a_N	$a_{\beta,P}$	a_N	$a_{\beta,P}$	a_N	$a_{\beta,P}$	a_N	$a_{\beta,P}$	a_N	$a_{\beta,P}$
1	n-pentane	15.15	[f]	[f]	13.43	51.15	13.53	47.77	13.12	52.39	13.67	47.18	13.06	52.54	13.26	49.34	13.07	51.50	13.10	52.86
2	*n*-hexane	15.22	14.80	40.80	13.54	50.96	13.45	47.77	13.12	52.39	13.41	46.79	13.12	52.73	13.29	48.63	13.19	51.74	13.19	52.76
3	CHex	15.19	[f]	[f]	13.52	51.17	13.45	47.86	13.12	52.23	13.42	46.86	13.18	52.72	13.33	48.82	13.12	51.49	13.09	52.95
4	*n*-octane	15.22	[f]	[f]	13.57	51.13	13.53	47.94	13.12	52.48	13.48	46.98	13.06	52.79	13.33	48.82	13.08	51.51	13.09	52.86
5	benzene	15.53	14.40	35.80	13.86	49.87	13.70	46.95	13.37	50.74	13.67	46.09	13.37	51.11	13.57	47.12	13.24	49.51	13.29	52.18
6	toluene	15.46	14.40	36.60	13.96	50.06	13.61	47.03	13.28	50.99	13.67	46.21	13.24	51.30	13.54	47.22	13.31	49.77	13.38	52.18
7	*t*-BuPh	15.47	[f]	[f]	13.77	50.45	13.61	47.36	13.28	51.49	13.54	46.34	13.24	51.73	13.50	47.63	13.31	50.35	13.29	52.47
8	PhBr	15.57	[f]	[f]	13.77	48.81	13.70	46.04	13.45	50.00	13.67	45.38	13.43	50.43	13.61	46.90	13.31	48.61	13.38	51.41
9	Pyridine	15.66	14.90	32.00	13.96	48.52	13.78	45.3	13.53	49.26	13.74	44.93	13.49	49.57	13.76	46.10	13.43	47.69	13.48	50.83

10	AcPh	15.64	f	f	13.96	48.52	13.78	45.3	13.53	49.51	13.80	44.99	13.55	49.69	13.74	46.15	13.49	47.77	13.38	50.93
11	t-BuPh/ CH$_2$Cl$_2$	15.61	f	f	13.86	48.62	13.70	45.96	13.53	49.42	13.80	44.80	13.49	49.81	13.74	46.15	13.54	47.92	13.48	50.93
12	CH$_2$Cl$_2$	15.77	f	f	14.06	47.95	13.86	44.55	13.61	48.76	13.80	44.10	13.61	49.13	13.88	45.77	13.54	47.11	13.48	50.26
13	DCE	15.71	f	f	13.96	47.68	13.86	44.55	13.53	48.68	13.74	44.03	13.55	49.13	13.79	45.74	13.49	47.03	13.38	50.06
14	CHCl$_3$	15.77	f	f	14.25	48.52	13.94	45.55	13.61	49.51	13.93	44.8	13.68	50.19	13.92	46.19	13.61	48.39	13.58	51.32
15	CCl$_4$	15.40	14.70	38.20	13.86	50.64	13.70	47.69	13.28	51.98	13.67	46.61	13.30	52.41	13.48	48.21	13.24	51.24	13.29	52.76
16	DME	15.27	f	f	13.86	49.49	13.61	46.37	13.37	50.66	13.67	45.70	13.30	50.74	13.63	47.12	13.31	49.19	13.29	51.51
17	Et$_2$O	15.24	f	f	13.58	50.26	13.53	47.11	13.20	51.65	13.61	46.47	13.12	51.8	13.43	48.24	13.08	50.58	13.19	52.38
18	i-Pr$_2$O	15.23	f	f	13.58	50.58	13.53	47.36	13.20	51.90	13.45	46.66	13.49	52.23	13.40	48.48	13.31	50.93	13.09	52.28
19	n-Bu$_2$O	15.36	f	f	13.86	50.64	13.53	47.28	13.20	51.82	13.42	46.53	13.18	52.23	13.40	48.18	13.24	50.87	13.29	52.66
20	Met-BuO	15.32	f	f	13.67	50.06	13.53	47.03	13.28	51.49	13.67	46.53	13.3	51.80	13.46	48.04	13.24	50.41	13.19	52.18
21	14D	15.45	f	f	13.86	49.49	13.78	46.12	13.45	50.41	13.74	45.25	13.43	50.74	13.70	46.63	13.37	49.13	13.38	51.7
22	THF	15.47	14.80	35.90	13.58	49.58	13.61	46.62	13.28	51.07	13.54	46.09	13.24	51.24	13.57	47.57	13.19	49.77	13.29	51.8
23	AcOEt	15.60	f	f	13.87	49.82	13.70	46.54	13.37	50.91	13.67	45.70	13.37	50.99	13.62	47.26	13.37	49.51	13.38	51.8
24	acetone	15.62	f	f	13.99	48.76	13.70	45.55	13.45	49.92	13.67	45.06	13.37	50.00	13.72	46.45	13.49	48.14	13.38	51.03

25	ACN	15.76	15.00	31.00	14.03	47.43	13.94	44.06	13.61	48.35	13.86	43.65	13.55	48.33	13.90	45.12	13.61	46.29	13.58	49.97
26	MeNO$_2$	15.86	16.00	28.60	14.07	47.04	14.03	43.56	13.70	47.94	13.99	43.26	13.61	48.02	13.99	44.93	13.54	45.83	13.28	49.49
27	DMSO	15.77	*f*	*f*	14.07	47.88	14.03	44.64	13.61	48.76	13.93	44.03	13.61	48.64	13.95	45.35	13.54	46.99	13.48	50.64
28	F	16.20	*f*	*f*	14.25	46.41	14.40	42.50	14.11	46.12	14.38	41.85	14.05	45.98	14.43	44.16	14.24	46.53	13.96	48.62
29	NMF	15.77	*f*	*f*	14.25	48.42	14.20	42.82	13.70	46.87	13.99	42.62	13.68	46.60	14.01	44.50	13.66	44.56	13.67	49.00
30	DMF	15.67	14.80	32.20	14.25	48.71	13.78	44.97	13.53	49.18	13.80	44.54	13.49	49.13	13.84	45.70	13.43	47.22	13.48	50.74
31	MeOH	16.20	15.70	21.90	14.32	47.79	14.03	44.31	13.78	48.43	14.56	44.03	13.74	48.27	14.07	45.48	13.77	46.64	13.67	50.93
32	EtOH	16.08	15.60	24.00	14.14	48.58	13.94	45.05	13.61	49.26	13.93	44.87	13.68	49.2	13.93	46.02	13.66	47.57	13.58	51.61
33	TFE	16.78	*f*	*f*	15.03	48.45	14.60	44.31	14.27	48.10	14.51	43.58	14.23	48.14	14.62	45.99	14.24	46.53	14.07	50.35
34	*i*-PrOH	16.04	15.20	27.60	14.06	49.39	13.86	45.71	13.61	50.00	13.74	45.44	13.61	50.00	13.88	46.59	13.66	48.61	13.48	52.09
35	*n*-BuOH	16.04	15.40	24.80	14.25	48.62	13.86	45.30	13.61	49.67	13.86	45.06	13.61	49.81	13.85	46.25	13.66	48.15	13.48	51.99
36	*t*-BuOH	15.91	*f*	*f*	13.96	49.68	13.94	46.21	13.61	50.58	13.80	46.02	13.55	50.80	13.83	47.11	13.54	49.54	13.48	52.09
37	BnOH	16.29	*f*	*f*	14.44	48.33	14.11	44.97	13.78	48.52	14.12	44.42	13.77	48.89	14.15	45.51	13.74	47.03	13.67	51.22
38	EG	16.30	*f*	*f*	14.54	47.85	14.27	44.31	13.86	48.02	14.31	43.58	13.86	48.02	14.26	45.45	13.77	46.18	13.86	50.93
39	TEG	15.30	15.50	22.90	14.25	48.43	14.03	45.13	13.70	48.93	13.99	44.42	13.8	49.13	13.80	45.67	13.66	46.99	13.86	51.03

Please do not adjust margins

40	water/MeOH	16.72	*f*	*f*	15.02	48.14	14.60	44.47	14.27	47.94	14.40	43.39	14.17	47.77	14.60	45.51	14.24	46.18	14.06	50.83
41	water	16.99	16.50	22.80	15.31	47.75	14.93	44.47	14.69	46.95	14.96	43.07	14.6	46.78	14.93	45.37	14.58	45.37	14.35	50.35
42	Buffer	*f*	*f*	*f*	*f*	*f*	*f*	*f*	*f*	*f*	14.96	43.13	14.6	46.84	*f*	*f*	*f*	*f*	14.35	50.35
43	AcOH	16.19	*f*	*f*	14.52	49.13	14.11	45.22	13.78	49.59	14.13	44.42	13.74	49.57	14.11	46.21	13.74	47.90	13.77	51.7
44	Et$_3$N	15.32	*f*	*f*	13.59	50.67	13.53	47.53	13.20	52.23	13.22	46.40	13.3	52.41	13.33	48.22	13.08	51.27	13.09	52.57
45	*i*-Pr$_2$NH	15.36	*f*	*f*	13.96	50.64	13.53	47.36	13.28	51.90	13.54	46.79	13.12	52.10	13.40	48.18	13.43	51.04	13.38	52.47
46	*i*-PenOH	15.96	*f*	*f*	*f*	*f*	*f*	*f*	*f*	*f*	*f*	*f*	*f*	*f*	*f*	*f*	*f*	*f*	*f*	*f*
47	CS$_2$	15.37	*f*	*f*	*f*	*f*	*f*	*f*	*f*	*f*	*f*	*f*	*f*	*f*	*f*	*f*	*f*	*f*	*f*	*f*
48	Mecyc	*f*	14.50	39.80	*f*	*f*	*f*	*f*	*f*	*f*	*f*	*f*	*f*	*f*	*f*	*f*	*f*	*f*	*f*	*f*
49	PhCl	15.56	*f*	*f*	*f*	*f*	*f*	*f*	*f*	*f*	*f*	*f*	*f*	*f*	*f*	*f*	*f*	*f*	*f*	*f*

[a] a_N and $a_{\beta,P}$ given in G.

[b] CHex: *cyclo*hexane, *t*-BuPh: *tert*-butylbenzene, PhBr: bromobenzene, AcPh: acetophenone, DCE: 1,2-dichloroethane, DME: 1,2-dimethoxyethane, 14D: 1,4-dioxane, THF: tetrahydrofurane, AcOEt: ethyl acetate, ACN: acetonitrile, DMSO: dimethylsulfoxide, F: formamide, NMF: *N*-methylformamide, DMF: *N,N*-dimethylformamide, TFE: 2,2,2-trifluoroethanol, EG: ethylene glycol, TEG: triethylene glycol, AcOH: acetic acid, *i*-PenOH: *iso*-pentanol, Mecyc: methylcyclopentane, PhCl: chlorobenzene, Buffer: Phosphate buffer at pH = 7.2.

[c] See refs. 9 and 17. [d] See ref. 12. [e] See ref.17. [f] Not available.
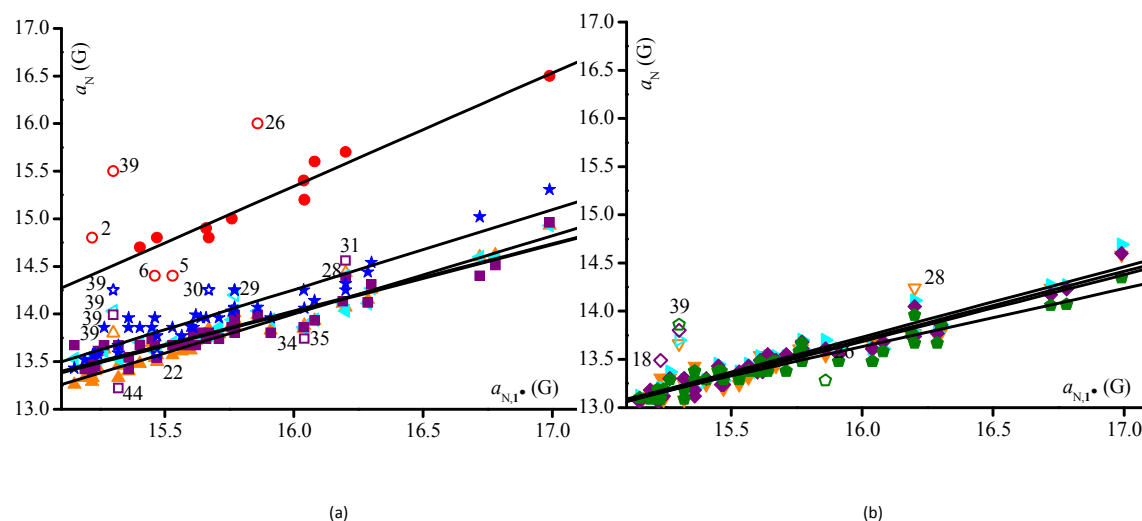
Journal Name

ARTICLE

Figure 5. Correlations $a_{N,1\bullet}$ vs a_N for (a) **2•** (●), **3•** (★), **4c•** (◄), **5c•**(■), and **6c•** (▲), and (b) **4t•** (►), **5t•**(◆), **6t•** (▼) and **7t•** (●). Empty symbols are for outliers.

All nitroxides displayed in Figure 1 exhibit the expected 6-line EPR signal due to the coupling between the nuclear spins of the nitrogen atom ($I_N = 1$) and phosphorus atom ($I_P = \frac{1}{2}$) and the odd electron on the nitroxyl moiety. Signals were recorded in more than 40 solvents. Nitrogen and β-phosphorus hyperfine coupling constants (hcc) a_N and $a_{\beta,P}$ for **1•** – **7t•** are collected in Table 1 excepted for **2'•** and **2"•**.

Non-specific properties of the solvent.

Among the non-specific solvent properties available – dipolar moment μ, relative permittivity constant ε_r, viscosity η and refractive index n –, only μ and ε_r were tested, as they were related to the polarity of the solvent (Table 1SI). As already reported for **1•**,[17] scattered plots were observed with μ and ε_r, like with a_N and $a_{\beta,P}$ for **3•** - **7t•** (Figure 1SI).[♩] Nevertheless, two trends were observed: a_N increased with increasing μ and ε_r, i.e., with increasing polarity, and $a_{\beta,P}$ decreased with increasing μ and ε_r.

Correlation of a_N and $a_{\beta,P}$ with benchmark hccs.

As **1•** was the nitroxide used in the first extensive study of solvent effects,[9] its a_N values are considered as benchmark values to investigate the solvent effect.[1,2] In 1976, **2•** was used in the first extensive solvent study (18 solvents) for nitroxides carrying a phosphorus atom at position β.[12]

The plots of a_N for **3•** - **7t•** against a_N for **1•** (benchmark molecule, eq. (2)) show that **3•** - **7t•** experience a weaker

solvation effect on their nitroxyl moieties than **1•** does. Thus, **4c,t•**, **5c,t•**, and **6t•** experience a similar solvent effect (same slopes α_1 in eq. (2c-f,h, Table 2SI) although weaker than for **3•** and **6c•**, and stronger than for **7t•**. TEG (39) is an outlier for all nitroxides, likely due to its high viscosity affording a peculiar solvation of the nitroxyl moiety. At this time, there is no rationale to take into account the other outliers.

$$a_N = y_0 + \alpha_1 \cdot a_{N,1\bullet}$$

(2)

The plots a_N of **4•** - **7t•** against a_N of **3•**, selected as the reference for the nitroxides carrying a phosphoryl group (eq. (3)), show that the nitroxyl moieties of **4c,t•**, **5c,t•** and **6t•** experienced the same solvation effect as **3•** did (Figure 6 and Table 3SI). On the other hand, **6c•** experienced a stronger solvation effect whereas **7t•** experienced a weaker solvation effect. There is no rationale to take into account solvents F (28), i-Pr$_2$NH (45), n-Bu$_2$O (19), and DMF (30) as outliers. Interestingly, for most nitroxides, EG (38) and TEG (39) are outliers, likely due to their high viscosity. For **5c•**, MeOH (31) and Et$_3$N (44) are also outliers.

$$a_N = y_0 + \alpha_2 \cdot a_{N,3\bullet}$$

(3)

Journal Name

ARTICLE

(a)

(b)
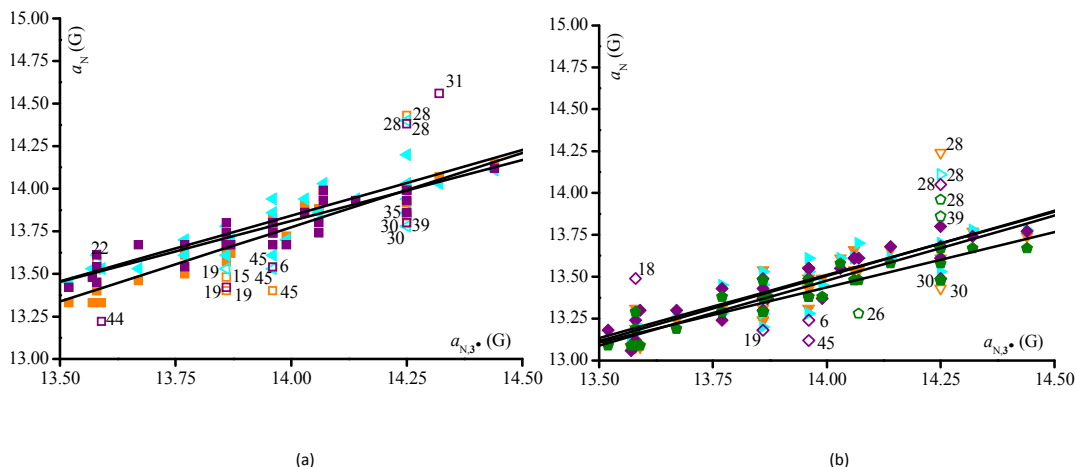
Figure 6. Correlations $a_{N,3\bullet}$ vs a_N for (a) **4c**• (◀), **5c**•(■), and **6c**• (▲), and (b) **4t**• (▶), **5t**•(◆), **6t**• (▼) and **7t**• (⬟). Empty symbols are for outliers.
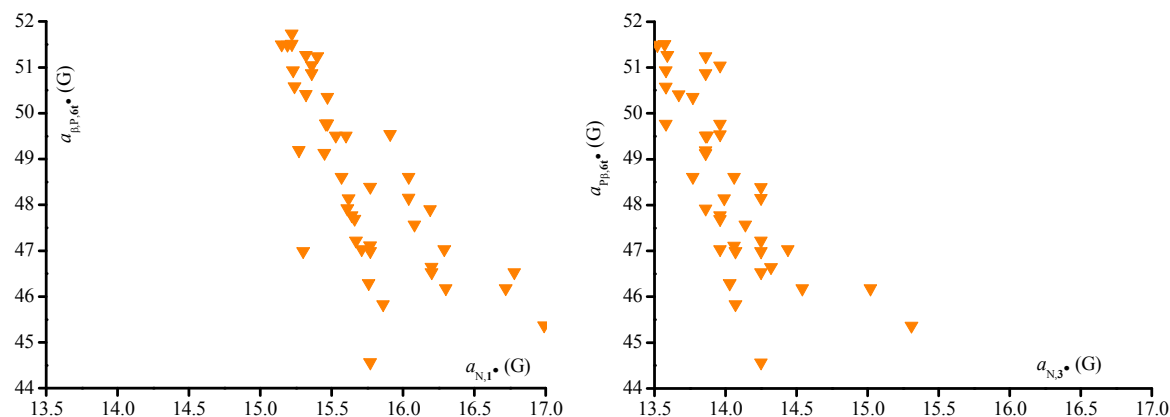
Figure 7. Plots $a_{N,1\bullet}$ vs $a_{\beta,P,6t\bullet}$ (left) and $a_{N,3\bullet}$ vs $a_{\beta,P,6t\bullet}$ (right), as examples.

(a)

(b)
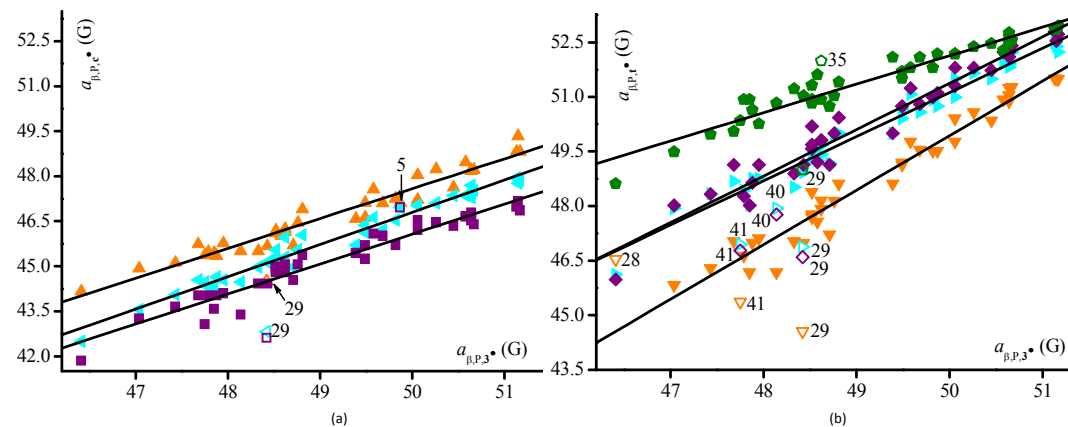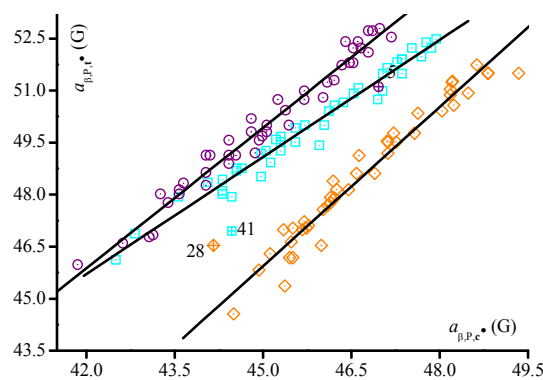
(c)

Figure 8. (a) Plots $a_{\beta,P,3\bullet}$ *vs* $a_{\beta,P}$ for **4c•** (◀), **5c•** (■), and **6c•** (▲). (b) Plots $a_{\beta,P,3\bullet}$ *vs* $a_{\beta,P}$ for **4t•** (▶), **5t•** (◆), **6t•** (▼),and **7t•** (⬤). (c) Plots $a_{\beta,P,c\bullet}$ *vs* $a_{\beta,P,t\bullet}$ for **4** (☐), **5** (⊙), **and** 6 (◇). Empty symbols are for outliers in (a) and (b). Crossed symbols are for outliers in (c).

The plots $a_{N,1\bullet}$ *vs* $a_{\beta,P}$ and $a_{N,3\bullet}$ *vs* $a_{\beta,P}$ exhibit a decrease in $a_{\beta,P}$ with increasing a_N values, in sharp contrast to the expectations from eq. 1 (Figure 7).♪ However, a broad scattering was observed whatever the reference used, implying that the solvation of the nitroxyl moiety has a different impact depending on the nitroxide, as exemplified with **6t•** (Figure 7). Thus, **3•** was selected as reference as it is the first 5-membered ring of this series, i.e. 3 methyl and one diethoxyphosphoryl group at position β. Good correlations were observed for **4c•** - **6c•** (eq. (4), Table 4SI, Figure 8) and **4t•** - **7t•** (eq. (5), Table 5SI, Figure 8) with a few outliers. That is, mainly NMF (29) for **4c•** - **6c•**, and NMF (29) and water (41) for **4t•** - **7t•**. Interestingly, **3•** and **4c•-6c•** experienced the same solvent effect, as shown by the very close values of their slopes (Table 4SI). On the other hand, a stronger effect (Table 5SI) was observed for **4t•-6t•**, implying more important conformational changes, in contrast to **7t•**.

$$a_{\beta,P,c} = y_0 + \alpha_3 \cdot a_{\beta,P,3\bullet}$$

(4)

$$a_{\beta,P,t} = y_0 + \alpha_4 \cdot a_{\beta,P,3\bullet}$$

(5)

$$a_{\beta,P,t\bullet} = y_0 + \alpha_5 \cdot a_{\beta,P,c\bullet}$$

(6)

$$a_N = y_0 + \alpha_7 \cdot E_T^N$$

(7)

$$a_{\beta,P} = y_0 + \alpha_8 \cdot E_T^N$$

(8)

Interestingly, when the $a_{\beta,P}$ of the diastereoisomers are plotted against each other, very good correlations are observed (Figure 8c). They show that the conformational changes are different from one diastereoisomer to the other (Table 6SI) and always afford a θ value smaller for the *trans* configuration than for the *cis* configuration (vide infra). Noteworthily, only a few outliers were observed, i.e., water (41) for **4•**, benzene (5) for **5•**, formamide (28) for **6•**.

Solvent effect on a_N and $a_{P\beta}$ in the cybotactic region.

The cybotactic effect of 45 solvents was investigated for each diastereoisomer separately (Table 1). Correlations of a_N and $a_{P\beta}$ with non-specific solvent parameters such as the dipole moment μ, the relative constant ε_r, and the refractive index n afforded only scattered plots (see SI). Thus, we investigated the specific solvent parameters related to the Hydrogen Bonding Donating (HBD) property α,♠ the intrinsic volume V_X, the cohesive pressure c (square of the Hildebrand solubility parameter δ), the molar volume V_M, and the normalized Reichardt polarity solvent parameter E_T^N (all these values are reported in Table 1SI). Except for E_T^N, all parameters afforded scattered plots, both for a_N and $a_{P\beta}$. Although scattering seems weak in Figure 9 and Figure 10 for the plots E_T^N *vs* a_N or $a_{\beta,P}$, respectively, it is still strong for **3•** - **7t•** ($R^2 < 0.90$, eqs. (7)c-j and (8b-i in Table 2 and Table 3, respectively), even after several outliers have been removed.

Amazingly, two correlations are possible for **3•** and **7t•** (eqs. (8b,c and j,k), respectively, in Table 3) affording good statistical outputs and different parameters, provided at least 10 solvents are removed! This highlights very nicely that E_T^N is not a suitable parameter to describe the solvent effect on $a_{\beta,P}$.

Journal Name

ARTICLE
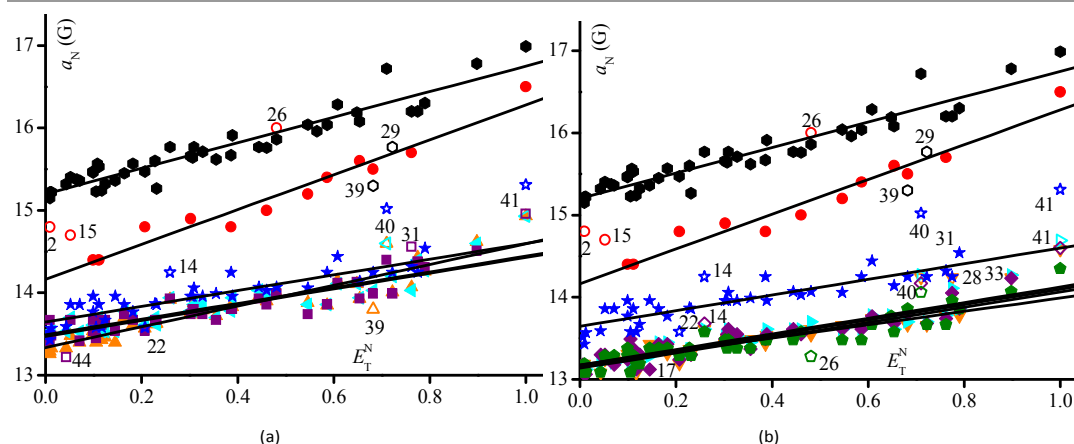
Figure 9. Plots E_T^N vs a_N for (a) **1•** (⬢), **2•** (●), **3•** (★), **4c•** (◄), **5c•**(■), and **6c•** (▲), (b) **1•** (⬢), **2•** (●), **3•** (★), **4t•** (►), **5t•**(◆), **6t•** (▼) and **7t•** (⬟). Empty symbols are for outliers.

Table 2. Correlations for a_N vs E_T^N for **1•** - **7t•** in various solvents

Eq.	Nitroxide	Slope α_7	Error[a]	y-intercept	Error[a]	R^{2b}	N^c	outliers
(7a)	**1•**	1.55	8	15.20	3	0.90	44	29,39
(7b)	**2•**	2.12	15	14.16	8	0.96	12	2,15,26
(7c)	**3•**	0.95	8	13.64	3	0.81	36	14,22,40,41
(7d)	**4c•**	0.95	6	13.49	3	0.85	41	40,41
(7e)	**4t•**	0.95	6	13.17	2	0.86	41	40,41
(7f)	**5c•**	0.96	7	13.47	3	0.81	40	31,41,44
(7g)	**5t•**	0.94	6	13.16	3	0.84	40	14,40,41
(7h)	**6c•**	1.26	7	13.33	3	0.88	41	39,40
(7i)	**6t•**	0.81	5	13.18	2	0.86	38	17,28,33,40,41
(7j)	**7t•**	0.93	6	13.13	3	0.86	41	26,40

[a] Error given on the last digit. [b] Square of the regression coefficient. [c] Number of data
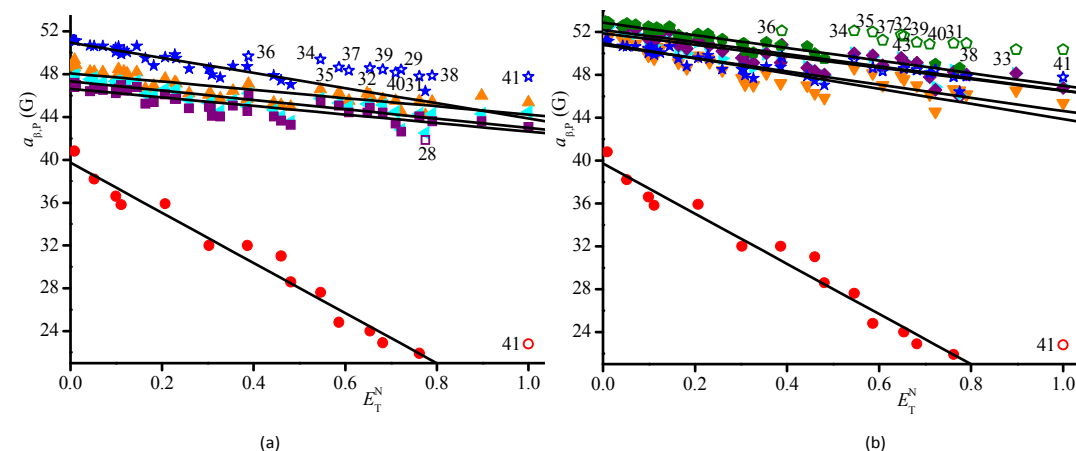
Figure 10. Plots E_T^N vs $a_{\beta,P}$ for (a) **2•** (●), **3•** (★), **4c•** (◄), **5c•**(■), and **6c•** (▲), (b) **2•** (●), **4t•** (►), **5t•**(◆), **6t•** (▼) and **7t•** (⬟). Empty symbols are for outliers.

Table 3. Correlations for $a_{\beta,P}$ vs E_T^N for **2•** - **7t•** in various solvents.

eq.	nitroxide	Slope α_8	error^a	y-intercept	error^a	R^{2b}	N^c	outliers
(8a)	**2•**	-23.84	107	39.96	45	0.98	16	41
(8b)	**3•**	-7.09	50	50.94	14	0.88	29	29,31,32,34-41
(8c)		-3.47	23	50.70	11	0.94	30	8-10,12-14,25-28
(8d)	**4c•**	-4.37	42	47.35	19	0.72	43	none
(8e)	**4t•**	-5.34	44	51.85	20	0.77	43	none
(8f)	**5c•**	-3.99	38	46.62	17	0.73	42	28
(8g)	**5t•**	-5.64	43	52.17	19	0.81	42	28
(8h)	**6c•**	-3.86	41	48.08	19	0.69	43	none
(8i)	**6t•**	-6.16	54	50.78	25	0.75	43	none
(8j)	**7t•**	-5.89	30	52.86	9	0.92	31	31-41,43
(8k)		-2.17	18	52.67	8	0.84	29	8-14,16,24-30

^{a} Error given on the last digit. ^{b} Square of the regression coefficient. ^{c} Number of data
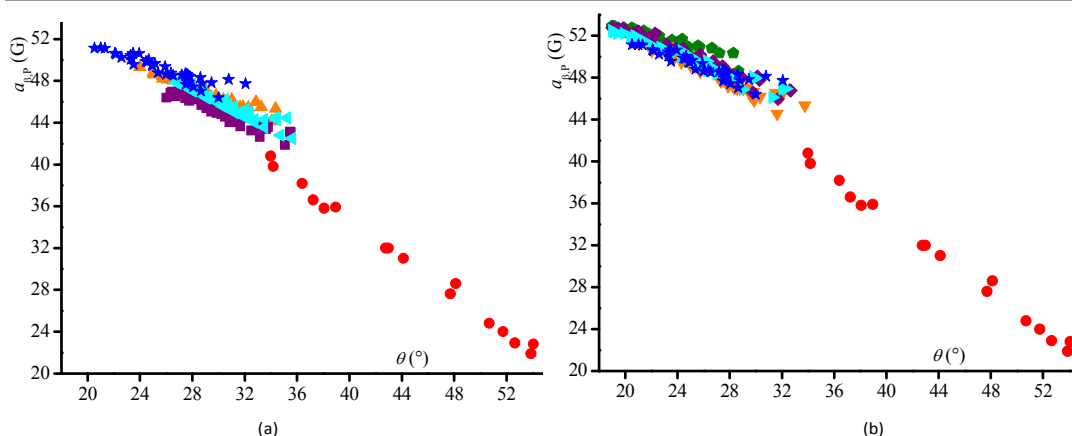
Figure 11. Plots θ vs $a_{\beta,P}$ for (a) **2•** (●), **3•** (★), **4c•** (◄), **5c•**(■), and **6c•** (▲), (b) **2•** (●), **3•** (★), **4t•** (►), **5t•**(♦), **6t•** (▼) and **7•** (⬟).

Table 4. $a_{\beta,Pmax}$ and the corresponding a_N, $a_{\beta,Pmin}$ and the corresponding a_N, diehedral angle θ_1, θ_{max} and the difference $\Delta\theta$ in their corresponding solvents for nitroxides **2•** - **7t•**.

nitroxide	solvent	$a_{\beta,Pmax}$ (G)	a_N (G)	θ_1 (°)^a	solvent	$a_{\beta,Pmin}$ (G)	a_N (G)	θ_{max} (°)^b	$\Delta\theta$ (°)^c
2•	n-hexane	40.80	14.80	34	MeOH	21.90	16.20	54	20
3•	cyclohexane	51.17	13.52	21	Formamide	46.41	14.25	32	11
4c•	n-octane	47.94	13.53	27	Formamide	42.50	14.40	36^d	9
4t•	n-octane	52.48	13.12	19	Formamide	46.12	14.11	32	12
5c•	n-pentane	47.18	13.67	27^e	Formamide	41.85	14.38	36	10
5t•	n-octane	52.79	13.06	19	Formamide	45.98	14.05	33	14
6c•	n-pentane	49.34	13.26	24	Formamide	44.16	14.43	34	10
6t•	n-hexane	51.74	13.19	21	NMF^f	44.56	13.66	34	13
7t•	cyclohexane	52.95	13.09	19	Formamide	48.62	13.96	29^d	10

^{a} θ_1 corresponds to θ_{min} unless otherwise mentioned. ^{b} Given in water unless otherwise mentioned. ^{c} $\Delta\theta = \theta_{max} - \theta_{min}$. ^{d} Given in Formamide. ^{e} In Et$_3$N, $\theta_{min} = 26°$. ^{f} NMF = N-methyl formamide.

Dihedral angle changes.

As mentioned in the introduction, the coupling with the atom at position β is given by the Heller-McConnell relationship (equation (1)) which in turn depends on the spin density on the nitrogen atom ρ_N^π, straightforwardly related to a_N, and to the dihedral angle θ between the bond of the atom at position β and the p-shape orbital on the N atom. Years ago,[28,29] it was shown that $\rho_N^\pi \cdot B_1$ in an apolar solvent such as n-hexane is around 59 G for the diethoxyphosphoryl group at position β of the nitroxyl moiety. Then, using eq. (1) it was possible to determine θ_1 for each nitroxide in the solvent exhibiting the

largest $a_{\beta,P}$ value. Thus, applying eq. (9), θ values were determined for each nitroxide in each solvent and in Figure 11. The main features – solvents, lowest and highest values of a_N, $a_{\beta,P}$ and θ, and its variation $\Delta\theta$ – are stored in Table 4.

$$\frac{a_{P,1}}{a_{P,n}} = \frac{a_{N,1}}{a_{N,n}} \cdot \frac{\cos^2\theta_1}{\cos^2\theta_n}$$

(9)

Interestingly (Table 4), a difference in $a_{\beta,P}$ of ca. 1G between **5t•** and **6t•** is accounted for by a difference of 2° in θ. The largest values of $a_{\beta,P}$ are reported in solvents with E_T^N lower than 0.01. The largest value is not always ascribed to the same solvent. However, the difference in $a_{P\beta}$ between solvents is negligible, i.e., less than 0.3 G. Except for **2•** and **6t•**, $a_{\beta,Pmin}$ values are reported in formamide whereas the corresponding θ_{max} are given in water, except for **4c•** and **7t•**. This denotes solvent effects strongly dependent on the structure of the nitroxide. $\Delta\theta$ varies from 9° to 14°, whatever the difference in $a_{\beta,Pmax}$ and $a_{\beta,Pmin}$ for **3•** - **7t•** (Table 4). This denotes very similar conformations and conformational changes for both *cis* and *trans* series. Amazingly, the highest values observed for θ_{max} for **3•** - **7t•** are similar to the lowest value observed for θ for **2•**, meaning that the bond rotations in **3•** - **7t•** are restricted.

Multiparameter correlations.

As several outliers and significant scatterings were observed when mono-parameter correlations were performed, multi-parameter relationships based on the Koppel– Palm (KP) and the Kalmet–Abboud–Taft (KAT) relationships (eqs. (10) and (11), and eqs. (15) and (16), respectively)♣ were tested with a_N

and $a_{P\beta}$. The KP relationship is a 6-parameter relationship combining two non-specific parameters – the polarizability parameter based on the refractive index n, given by the Lorenz-Lorentz function (eq. (12)), and the polarity parameter, based on the relative permittivity ε_r, given by the Kirkwood function (eq. (13)) – and four solvent specific parameters – the solvent basicity/nucleophily parameter B, the solvent acidity/electrophily parameter E, the Hildebrand's solubility parameter δ_H, and the molar volume V_M of the solvent. The values of E were determined using eq. (14) based on the Kirkwood (eq. (13)) and Lorentz-Lorentz (eq. (12)) functions and the Dimroth-Reichardt polarity parameter $E_{T,30}$.

$$\log a_N = \log a_{N,0} + a_1 \cdot f(n^2) + a_2 \cdot f(\varepsilon_r) + a_3 \cdot B + a_4 \cdot E + a_5 \cdot \delta_H^2 + a_6 \cdot V_M$$

(10)

$$\log a_{\beta,P} = \log a_{\beta,P_0} + b_1 \cdot f(n^2) + b_2 \cdot f(\varepsilon_r) + b_3 \cdot B + b_4 \cdot E + b_5 \cdot \delta_H^2 + b_6 \cdot V_M$$

(11)

$$f(n^2) = \frac{(n^2-1)}{(n^2+2)}$$

(12)

Table 5. Koppel-Palm linear correlations of a_N for **1•** - **8•**.

eq.	nitroxide	y-intercept[a]	a_4[a,b]	a_5[a,b]	R^2[c]	N[d]	F-test[e]	w_E[f]	w_c[f]	outliers
(10a)	**1•**[g]	14.82 (14)	0.056 (2)	-[h]	0.94	41	280	89	11[i]	29,39
(10b)	**2•**[j]	15.09 (44)	0.058 (6)	-[h]	0.93	15	82	86	14[i]	2,15,26
(10c)	**3•**	13.55 (4)	0.017 (6)[k]	0.0006 (1)[l]	0.88	28	95	34	66	14,28
(10d)	**4c•**	13.46 (2)	0.020 (4)	0.0004 (1)	0.91	39	182	48	52	33
(10e)	**4t•**	13.12 (3)	0.020 (10)	0.0004 (1)	0.90	39	171	48	52	33
(10f)	**5c•**	13.43 (3)	0.027 (4)	0.0003 (1)[m]	0.89	37	135	62	38	31,44
(10g)	**5t•**	13.11 (3)	0.028 (3)	0.0003 (1)[o]	0.90	38	154	65	35	14,18
(10h)	**6c•**	13.34 (3)	0.036 (4)	0.0002 (1)[p]	0.90	39	167	78	22	39
(10i)	**6t•**	13.09 (3)	0.022(4)	0.0004 (1)	0.90	39	160	51	49	33
(10j)	**7t•**	13.14 (3)	0.024 (3)	0.0002 (1)	0.86	33	96	68	32	none

[a] Errors are given on the last digit in parentheses. [b] Student t-test at 99.99% unless otherwise mentioned. [c] Square of the regression coefficient. [d] Number of data. [e] Student-Fischer F-test given at 99.99% unless otherwise mentioned. [f] Weight of each parameter in percent with an error of ± 7% as given by eqs. 18 and 19. [g] Polarizability was the only parameter affording reliable statistical outputs, i.e., a_1 = 1.61 (50) and t = 99.73%. [h] Not included in the correlation. [i] Given for $f(n^2)$. [j] a_1 = -2.39 (1.59) and t-test at 84%. Other possibilities were even worse. [k] t = 98.50%. [l] t = 99.00%. [m] t-test at 99.94%. [o] t-test at 99.90%. [p] t = 99.35%.

Table 6. Koppel – Palm multiparameter correlations (eq. (11)) based on the Kirkwood function of the relative permittivity ε_r, the cohesive pressure c (square of the Hildebrand solubility parameter δ), and on the molar volume V_M for nitroxides **4•** - **8•**.

eq		$\log a_{\beta,P,0}$[a]	b_2[a,b]	b_5[a,b]	b_6[a,b]	R^2[c]	F[d]	N[e]	$w_{f(cr)}$[f]	w_c[f]	w_{VM}[f]	outliers
(11a)	**3•**	50.4 (7)	-6.8 (12)	-[g]	0.014 (4)[h]	0.79	62	35	60		40	34
(11b)	**4c•**	47.8 (7)	-5.8 (12)	-0.0019 (5)[i]	0.012 (4)	0.87	82	39	41	34	25	41
(11c)	**4t•**	52.2 (8)	-5.6 (14)[i]	-0.0026 (5)	0.012 (5)[j]	0.86	74	39	36	41	23	41
(11d)	**5c•**	47.0 (7)	-4.3 (13)[k]	-0.0022 (5)[h]	0.009 (4)[l]	0.82	54	39	34	44	22	41
(11e)	**5t•**	52.7 (7)	-6.1 (13)	-0.0029 (5)	0.013(4)[m]	0.90	100	39	35	42	23	41
(11f)	**6c•**	48.6 (7)	-5.3 (13)[h]	-0.0016 (5)[n]	0.009 (4)[o]	0.82	55	39	44	33	23	41
(11g)	**6t•**	51.8 (11)	-10.4 (18)	-0.0009 (5)[p]	0.015 (6)[q]	0.82	54	40	56	19	25	none
(11h)	**7t•**	53.4 (7)	-5.2 (11)	-0.0018 (4)[r]	0.007 (4)[q]	0.89	63	28	45	38	17	31,32,34-36,38,41

[a] Errors are given on the last digit in parentheses. [b] Student t-test of confidence given at 99.99 % unless otherwise mentioned. [c] Square of the regression coefficient. [d] Student-Fischer F-test of reliability given at 99.99% confidence. [e] Number of data. [f] Weight of each parameter in per cent with an error of ± 7% as given by eqs. 18 and 19. [g] Not included in the correlation. [h] t = 99.90%. [i] t = 99.98%. [j] t = 99.00%. [k] t = 99.80%. [l] t = 97.40%. [m] t = 99.64%. [n] t = 99.95%. [o] t = 97.80%. [p] t = 91.70%. [q] t = 98.20%. [r] t = 99.96%.

Journal Name

ARTICLE

$$f(\varepsilon_r) = \frac{(\varepsilon_r - 1)}{(2\varepsilon_r + 1)}$$

(13)

$$E = E_{T,30} - 25.10 - 14.84 \cdot f(\varepsilon_r) - 9.59 \cdot f(n^2)$$

(14)

Whatever the combination of parameters – from one to six parameters – applied to the KP relationship (eq. (10) the basicity B, the molecular volume V_M and the polarizability $f(n^2)$ are useless to describe the effect of the solvent on a_N, except for **1•** for which a correlation is observed (eq. (10a) with E and $f(n^2)$ and not with $f(\varepsilon_r)$. For **2•**, only E is sufficient to describe the effect of the solvent (the occurrence of the polarizability $f(n^2)$ is 84% reliable, below the conventional statistical requirements (eq. (10b) in Table 7). The solvent effect for **3•** - **7t•** is described the acidity E and the cohesive pressure c (as an example see Figure 4SI). For **5c•** MeOH (31) and Et$_3$N (44) are outliers, for **5t•**, chloroform (14) and i-Pr$_2$O (18) are outliers, with no rationale at this time, and TEG (39) is outlier for **6c•** – likely due to its high viscosity.

Noteworthy, solvent effects in nitroxides **4•** - **6•** are also well described by the cohesive pressure c and the polarizability $f(\varepsilon_r)$ (see Table 7SI).

Whatever the combination of parameters – from one to six parameters – applied to the KP relationship (eq. (11**)**, the basicity B and polarizability $f(n^2)$ are useless to describe the effects of the solvent on $a_{\beta,P}$ (very poor statistical outputs). Surprisingly, the changes in $a_{\beta,P}$ of **2•** with the solvent cannot be described by eq. (11). Interestingly, $a_{\beta,P}$ for **4•** - **7t•** are described by a 3 parameter KP relationship: $f(\varepsilon_r)$ (polarity), c (cohesive pressure), and V_M (molar volume). Indeed, good statistical outputs are obtained with two parameters ($f(\varepsilon_r)$ and c) but the scattering is decreased when V_M is included (Figures 5SI and 6SI).$^{\lozenge}$ At the difference of **4•-7t•**, $a_{\beta,P}$ of **3•** are described by a two-parameter correlation: $f(\varepsilon_r)$ and V_M. Water (41) is the only outlier observed for KP relationships relying on $f(c,f(\varepsilon_r))$ or $f(c,f(\varepsilon_r),V_M)$. Water is a small molecule, it might occur that its effect might not be described using conventional molecular descriptors.[13,36,37] In the case of **6t•**, no outliers are observed when $f(\varepsilon_r)$, c, and V_M are used as parameters.

Solvent effects on a_N and $a_{\beta,P}$ are also described by the KAT relationships (eqs. (15) and (16), respectively) relying on 4-6 cybotactic parameters:[13] one non specific parameter π^* describing the polarity/polarizability effect, the discontinuous

polarizability correction term δ, the Hydrogen Bonding Acceptor (basicity) HBA property β and the Hydrogen Bonding Donor (acidity) property α. In some cases, cohesive pressure c is included in the KAT relationship. In our case, the intrinsic volume V_X, as given by McGowan,[38] was also included.

$$\log a_N = \log a_{N_0} + c_1(\pi^* + c_2 \cdot \delta) + c_3 \cdot \alpha + c_4 \cdot \beta + c_5 \cdot \delta_H^2 + (c_6 \cdot V_X)$$

(15)

$$\log a_{\beta,P_0} = \log a_{\beta,P_0} + d_1(\pi^* + d_2 \cdot \delta) + d_3 \cdot \alpha + d_4 \cdot \beta + d_5 \cdot \delta_H^2 + (d_6 \cdot V_X)$$

(16)

$$E_T^N = 0.36 \cdot \pi^* + 0.47 \cdot \alpha + 0.01$$

(17)

Whatever the combination of parameters – from one to six parameters – applied to the KAT relationship (eq. (15**)**): the HBA property β, the intrinsic molecular volume V_X, and the discontinuous polarizability correction term δ are useless to describe the effects of the solvent on a_N (very poor statistical outputs). The normalized Reichardt E_T^N encompasses three effects: polarity, polarizability, and HBD property α of the solvent (eq. (17)). As expected from eq. (17) and correlations $a_N = f(E_T^N)$ (Table 2), good correlations involving π^* and α are obtained and they are reported in Table 7. Nevertheless, the use of a 3-parameter correlation using c affords better statistical outputs (Table 7), which is observed as a decrease in the scattering (Figure 7SI). Interestingly, the use of c for the correlation of **4t•**, **5t•**, and **6t•** leads to suppress the outliers observed when two parameter correlations are applied. Several outliers are observed that are different for each nitroxide, and also different according to the type of correlation applied (2- (see Table 9SI) or 3-parameter correlations, except for **1•** and **2•**) and also different from those reported for $a_N = f(E_T^N)$ (Table 2).

Whatever the combination of parameters – from one to six parameters – applied to the KAT relationship (eq. (16)): the HBA property β and the discontinuous polarizability correction term δ are useless to describe the effects of the solvent on $a_{\beta,P}$ (very poor statistical outputs). As expected from correlations $a_{\beta,P} = f(E_T^N)$ and eq. (17), polarity/polarizability π^* and HBD property α are required to describe $a_{\beta,P}$ values.$^{\heartsuit}$ The biparameter (π^*,α) relationships are slightly improved when the intrinsic volume V_X is included, as exemplified with **6c•** (Figure 8SI). Interestingly, $a_{\beta,P}$ for **3•** are well described using either π^* and α or π^* and V_X (see Table 10SI) as parameters

whereas only a moderate correlation with π^* and V_X is observe for **7t•** (7 outliers in Table 8). Acetonitrile (25), nitromethane (26), formamide (28), *N*-methyl formamide (29, and water (41) are the most frequently observed outliers, with no rationale at this time.

Besides the absolute values of the coefficients of the KP and KAT relationships which describe the impact of each effect, the relative distribution given by their weight (*w* in %, eqs. 18 and 19) provides information on their relative importance.[39,40] The weight (eq. 18) of each effect depends on each parameter C_i – which are not on the same scale – and their respective weighted parameters α_i given in eq. 19. The latter depends on the average of each parameter and on the degree of freedom (number of data *N* and number of parameters *p*, eq. 19).

$$w = \frac{\alpha_i \cdot C_i}{\sum \alpha_i \cdot C_i}$$

(18)

$$\alpha_i = \sqrt{\frac{\sum_{i-1}^{N}\left(x_i - \bar{x_i}\right)^2}{N-(p-1)}}$$

(19)

Discussion

Preparation of nitroxides 4• - 6•.

Aziridines are analogues of epoxides, except that they are much less applied and are considered as ugly cousins.[41] Nevertheless, aziridines can readily react as epoxides do, when a strong electrowidthdrawing group is attached to the nitrogen atom. In our case, although weakly activated, aziridines turn

out to be versatile key intermediates affording an easy and diastereoselective access to nitroxides **4•** - **7t•** via the one-step addition of the azide and acetoxy groups (Scheme 5). The combination of the polar (electrowidthdrawing effect of the diethoxyphosphoryl group) and steric effects affords a selective addition of the nucleophile on the methylenic carbon. This approach is currently under development for the preparation of new nitroxides, for example those carrying thioalkyl or thioester groups.

General considerations on hccs.

For historical considerations,[9] a_N of **1•** are commonly accepted as the benchmark values all other a_N are compared with. As displayed in Figure 5 and Table 2SI, good correlations are reported ($R^2 > 0.85$) although several outliers are observed. Hence, a_N of **2•** to **7t•** experienced the same effect as that experienced by a_N of **1•** but to a different extent (Table 2SI), as highlighted by the slopes greater than 1 for **2•**, between 0.69 – 0.82 for **3•** - **6•**, and 0.6 for **7t•**. Better correlations are observed when a_N of **3•** is used as reference (Table 3SI and Figure 6). Interestingly, except **6c•** and **7t•** - slopes of ca. 0.87 and 0.66, respectively – all phosphorylated nitroxides experienced the same solvent effect, i.e., slope ≈ 0.7-0.8 (Table 3SI).
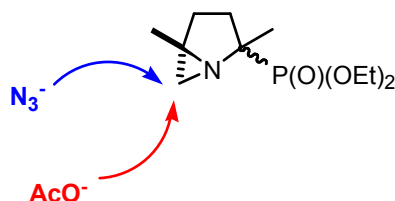
Scheme 5. Aziridine as versatile key intermediate in the preparation of **4•** - **6•**

Table 7. Kalmet – Aboud – Taft multiparameter correlations (eq. (15) for a_N of nitroxides **1•** - **8•** based on the polarity/polarizability parameter π^*, the cohesive pressure *c*, and on the Hydrogene Bonding Donor (HBD) parameter α of solvents.

eq.		*y*-intercept[a]	c_1[a,b]	c_3[a,b]	c_5[a,b]	R^2[c]	F[d]	N[e]	w_{π^*}[f]	w_α[f]	w_c[f]	outliers
(15a)	**1•**	15.18 (3)	0.49 (6)	0.68 (4)	0.0002 (6)[g]	0.96	281	41	30	58	12	29,39
(15b)	**2•**	14.00 (14)	1.05 (20)[h]	1.13 (9)	-[i]	0.96	103	12				2,15,26
(15c)	**3•**	13.57 (4)	0.55 (7)	0.41 (6)	-[i]	0.84	86	35	55	45		41
(15d)	**4c•**	13.41 (3)	0.29 (6)	0.23 (5)	0.0004 (1)	0.93	167	39	27	26	46	33
(15e)	**4t•**	13.07 (3)	0.35 (6)	0.34 (4)	0.0003 (1)	0.93	154	40	30	27	43	none
(15f)	**5c•**	13.34 (4)	0.36 (6)	0.35 (5)	0.0004 (1)	0.91	117	38	27	36	37	1,31
(15g)	**5t•**	13.09 (3)	0.33 (7)	0.35 (5)	0.0003 (1)[j]	0.90	108	40	30	37	33	none
(15h)	**6c•**	13.26 (3)	0.51 (6)	0.41 (4)	0.0002 (1)	0.95	227	39	39	42	19	39
(15i)	**6t•**	13.07 (3)	0.26 (7)[k]	0.38 (5)	0.0003 (1)	0.91	123	40	22	45	33	none
(15j)	**7t•**	13.09 (2)	0.29 (5)	0.25 (4)	0.0003 (1)	0.94	150	32	29	31	40	26,33

[a] Errors are given on the last digit in parentheses. [b] Student *t*-test of confidence given at 99.99% unless otherwise mentioned. [c] Square of the regression coefficient. [d] Student-Fischer *F*-test of reliability given at 99.99% confidence. [e] Number of data. [f] Weight of each parameter in percent with an error of ± 7% as given by eqs. 18 and 19. [g] *t* = 99.10%. [h] *t* = 99.94%. [i] Not used in the correlation. [j] *t* = 99.98%. [k] *t* = 99.96%.

Journal Name

ARTICLE

Table 8. Kalmet – Aboud – Taft multiparameter correlations (eq. (16) for $a_{\beta,P}$ of nitroxides **1•** - **8•** based on the polarity/polarizability parameter π^*, the intrinsic volume V_x, and on the Hydrogen Bonding Donor (HBD) parameter α of solvents.

eq		y-intercept[a]	d_1[a,b]	d_3[a,b]	t[b]	d_6[a,b]	t	R^{2c}	F^d	N^e	w_{π^*}[f]	w_{α}[f]	w_{Vx}[f]	outliers
(16a)	**2•**	40.52 (58)	-9.87 (93)	-12.86 (63)	99.99	_[g]	_[f]	0.98	297	14	34	66		41
(16b)	**3•**	51.00 (11)	-2.75 (20)	-0.56 (18)	99.55	_[g]	_[f]	0.91	146	30	81	19		12,13,25,26,28,31
(16c)	**4c•**	46.40 (49)	-2.94 (37)	-0.69 (28)[h]	98.30	1.60 (47)	99.82	0.84	60	39	57	18	25	41
(16d)	**4t•**	51.31 (38)	-3.44 (38)	-0.77 (21)[i]	99.91	1.15 (36)	99.96	0.91	117	38	63	19	18	28,29
(16e)	**5c•**	46.29 (31)	-2.45 (23)	-0.66 (17)[j]	99.95	0.69 (30)	97.10	0.90	97	35	63	23	14	5,25,26,28,29
(16f)	**5t•**	51.34 (40)	-3.44 (30)	-0.92 (22)[k]	99.98	1.43 (38)	99.94	0.91	121	38	58	21	21	28,29
(16g)	**6c•**	47.86 (36)	-3.24 (27)	-0.41 (20)[l]	95.00	0.96 (35)	99.00	0.89	96	39	71	12	17	41
(16h)	**6t•**	50.78 (40)	-4.26 (30)	-1.02 (22)	99.99	0.77 (40)	94.30	0.94	159	37	68	22	10	25,26,29
(16i)	**7t•**	52.23 (23)	-1.89 (18)	_[g]	_[g]	0.007 (2)	99.36	0.87	102	32	77		23	10,12,13,25,26,28,29

[a] Errors are given on the last digit in parenthesie. [b] Student t-test of confidence given at 99.99% unless otherwise mentioned. [c] Square of the regression coefficient. [d] Student-Fischer F-test of reliability given at 99.99% confidence. [e] Number of data. [f] Weight of each parameter in percent with an error of ± 7% as given by eqs. 18 and 19. [g] Not used in the correlation. [h] t = 98.30%. [i] t = 99.91%. [j] t = 99.95%. [k] t = 99.98%. [l] t = 95.00%.

Journal Name

ARTICLE
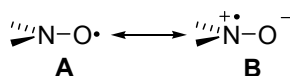
Figure 12. Mesomeric forms of the nitroxyl moiety

Figure 13. Canonical forms for the hybridization at the nitrogen atom of a nitroxyl moiety and % of character s in the SOMO.

Given by the EPR theory,[21] the hyperfine coupling on position α is directly related to the electron density localized on the nucleus, i.e., the Fermi contact term Q_N given in eq. (20). This term depends on the shape of the localized orbital describing the odd electron. That is, for π-radicals, the SOMO is of p-shape, i.e., a low s-character and then a low spin density in contact with the nucleus, and thus any increase in the s character will lead to an increase in electron density and, hence, to an increase in a_N.

$$a_x = cte \cdot Q_N$$

(20)

In the case of nitroxides, the electron density Q_N is controlled both by the presence of electron widthdrawing groups (EWG) – which favours form **A** over form **B** (Figure 12),[7,9,10] that is, Q_N decreases, a_N decreases – and by the hybridation (pyramidalization) at the nitrogen atom, varying from sp^3 to sp^2 (Figure 13), i.e., the higher the pyramidalization (form **C**), the higher the character s in the SOMO, the higher a_N and conversely.

Plots $a_{N,1\bullet}$ vs $a_{N,3\bullet-7t\bullet}$ (Figure 5) displayed 4 families (Table 2SI): **2•** with a slope greater than 1 implying higher accessibility of the nitroxyl moiety to the solvent despite the presence of EWG (vide infra), **3•** and **6c•** with a slope around 0.83, **4c•** - **5t•** and **6t•** exhibiting slopes close to 0.7 and **7t•** with a slope at 0.6. The slopes less than 1 for the other families were due to a subtle interplay of polar effect, steric hindrance and steric strain (vide infra). To suppress the ring strain, plots $a_{N,3\bullet}$ vs $a_{N,4\bullet-7t}\bullet$ were performed (Figure 6) showing 3 families: **4c•** - **5t•** and **6t•** with slopes between 0.7 – 0.8, **6c•** with a slope at 0.87, and **7t•** with a slope at 0.66, highlighting again the subtle interplay of steric hindrance and polarity effect as all exhibit lower solvation effect than **3•**, as **6c•** is better solvated than **6t•** although it exhibited the same polarity, and **7t•** the least efficiently solvated. Nevetherless, these results must be discussed cautiounly as 4-5 solvents were considered as outliers for each nitroxide.
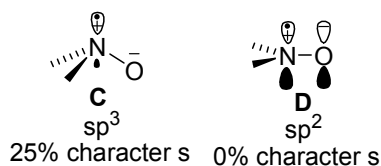
The Heller-McConnel relationship (1) shows that $a_{\beta,P}$ is directly proportional to the electron density ρ_N^π,[21] which, in turn, is expected to be linearly related to a_N, implying that increasing $a_{\beta,P}$ is expected with increasing a_N, provided no change in the hybridization or in the mode of solvation.[10,21] Hence, a decrease in $a_{\beta,P}$ is observed with increasing a_N (Table 1) leading to scattered plots between $a_{\beta,P}$ and both $a_{N,1\bullet}$ and $a_{N,3\bullet}$. (Figure 7). Thus, $a_{\beta,P}$ of **3•** was applied as reference for **4•** to **7t•** (Figure 8). Interestingly, **4c•-6c•** (Table 4SI and Figure 8) exhibit the same slope as **3•**, meaning that the solvation of the nitroxyl moiety has the same impact on their conformations. On the other hand, **4t• – 6t•** exhibit a higher impact whereas it is lower for **7t•** (Table 5SI).

Correlations based on the normalized Dimroth-Reichardt constants E_T^N.

The correlations a_N with E_T^N or $E_{T(30)}$ have been known since the work of Napier et al.[9] for **1•** and that of Il'Yasov and coll.[12] for **2•**. As recently reported,[17] the lower y-intercept for β-phosphorylated nitroxides than for **1•** is due to the presence of the strong EWG $P(O)(OEt)_2$ ($\sigma_I = 0.32$)[42] favouring form **A** over form **B** (Figure 12). Thus, the lower y-intercept for **4• - 7t•** than for **3•** is due to the presence of a second EWG. The lower y-intercept for the *trans* series than for the *cis* series is due to a more pronounced sp^2 character of the N atom in the *trans* series (Figure 13), denoting a larger strain. Recently we observed that the solvent effect (slope in eq. (7)) increased in series **3• < 1• < 2•** due to changes both in accessibility (steric hindrance) and in sensitivity (presence of EWG) of the nitroxyl moiety.[17] The polarity of nitroxides is estimated using the Hammett constant σ_I given as -0.06, 0.27, 0.27, 0.43, 0.43, 0.43, 0.43, 0.45, 0.45, and 0.44 for **1• - 7t•**, respectively. Hence, the nitroxides are gathered in 3 families of σ_I: **1•**, **2•** and **3•**, and **4• - 7t•**. The slope increases in the series: **6t• < 3•** ≈ **4•** ≈ **5•** ≈ **7t• < 6c• < 1• < 2•** meaning that the polarity does not play the major role. Thus, the slopes of **4•**, **5•**, and **7t•** are very close to that of **3•**, despite the presence of a second EWG, and this implies a change in the conformation affording a better access of the nitroxyl moiety to the solvent. For **6c•**

and **6t•**, the presence of strongly polar azide group implies strong repelling electrostatic interaction affording conformations exhibiting either a better (**6c•**) or a lesser (**6t•**) access of the nitroxyl moiety to the solvent than in **3•** - **5•**, and **7t•**. The lower slopes for **3•** - **7t•** than for **1•** are in part due to higher polarity of these nitroxides than **1•**.

The *y*-intercepts for the plots $a_{\beta,P}$ vs E_T^N, for $E_T^N = 0$, correspond to the $a_{\beta,P}$ values expected in *n*-pentane and *n*-hexane. Due to the significant scattering of the data, the error between expected and experimental data is around 0.5 G (Table 3). Nevertheless, several trends emerged. The *y*-intercept (Table 3) shows that the position of the diethoxyphosphoryl groups is similar in **3•** and in the *trans* series ($\theta \approx 20°$, Table 4) and smaller than in the *cis* series ($\theta \approx 25°$, Table 4), implying a better hyperconjugation effect and, hence, larger $a_{\beta,P}$ values for **3•** and the *trans* series.

Il'Yasov and coll.[12] showed that the $a_{\beta,P}$ of **2•** is temperature dependent, implying that the conformation of **2•** changes with the temperature, meaning that the rotation around the C—N bond is partly free. Although the rotations around the C—N bond are restricted in the 6-membered ring, the exchange of the methyl groups between the equatorial and axial positions in symmetrical **1•** has no effect on the solvation of the nitroxyl moiety. On the other hand, eq. (1) shows that $a_{\beta,P}$ depends on both the change in spin density given by ρ_N^π and the conformational changes given by θ, meaning either the slope in eq. (8) increases as expected with the increasing the solvent polarity as form **B** is favoured over form **A**, provided no change in conformation, i.e., $\Delta\theta \approx 0°$ or the slope decreases implying that the conformational changes, i.e., increasing θ values, overbalance the effect of the solvent polarity. Recently, we ascribed the solvent effect to a change of conformation for a negative slope. The trends observed in Table 3 shows that the influence of solvent increases in the series as the slopes decreases: **7t• > 3• ≈ 6c• ≈ 5c• ≈ 4c• > 4t• ≈ 5t• > 6t• > 2•**. It comes out that the solvent has the same effect for the *cis* series and **3•**. However, it is not possible to discuss quantitatively the influence of the polarity and the conformation changes on the slope.

Thus, applying eq. (9) affords some hints on the conformational changes through the variation in dihedral angle $\Delta\theta$ (Figure 11 and Table 4). Except for **2•** for which $\Delta\theta =$

20°, values of $\Delta\theta$ are centered at 12°±3. Interestingly, the distribution of the $\Delta\theta$ values is in good agreement with the slopes of eqs. (4) and **(5)**. Although such a small changes can have a clear effect on $a_{\beta,P}$ ($\Delta a_{\beta,P} \approx 2G$ for $\Delta\theta \approx 2°$), the change in conformation is not expected to be large enough to take into account the difference observed between the slopes.

Nevertheless, the negative slopes in eq. (8) mean that the increase in dihedral angle θ overmatches the increase in spin density ρ_N^π due to the increase in solvent polarity (vide supra). It is likely that the phosphoryl group is solvated in the same way for all nitroxides and the increase in polarity of the solvent favours form **F** (Scheme 6).

It has been noted that increasing the polarity of the solvent favours the mesomeric forms **B** and **F** of the nitroxyl and phosphoryl moieties, respectively (Figure 1 and Scheme 6), implying that the attractive dipole-dipole interaction between the positive P- and the negative O-atoms of the phosphoryl and the nitroxyl moieties, respectively, is the driving force leading to a change in the dihedral angle θ (Scheme 7).♦ Such a conformation change from a non polar to a polar solvent is expected to lead ultimately to the formation of a highly strained 4-membered ring of the azaoxaphosphetane type (Scheme 7).

Multiparameter approach. General considerations.

As mentioned above, significant scattering was observed for the plots a_N vs E_T^N and $a_{\beta,P}$ vs E_T^N. It led us to investigate the solvent effect through the Linear Solvation Energy Relationship[13,43] (LSER), as given by eq. (21), *A* and A_0 are the values of the solvent-dependent physico-chemical properties; the polarity/polarizability terms describe the solute/solvent dipole and induced dipole interactions: given, for example, by the Kirkwood functions $f(\varepsilon_r)$ (eq. (13)), by the Lorenz-Lorentz function $f(n^2)$ (eq. (12)), or by π^*; the hydrogen bonding terms describe the interaction HBD/HBA between the solvent and the solute: given for example, by α and β parameters as defined by Abraham,[13,36] or by *E* (electrophily/Lewis acidity) and *B* (nucleophily/Lewis basicity) as defined by Koppel and Palm:[44] and the bulk/cavity terms (*structuredness* of the solvent) describe the energy needed to form cavities for the solute molecules: given, for example, by the cohesive pressure c, V_M, or V_X.[13,36,37]
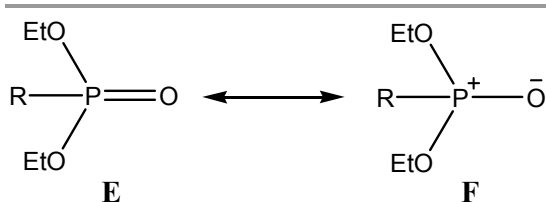
Scheme 6. Mesomeric forms for the phosphoryl group.
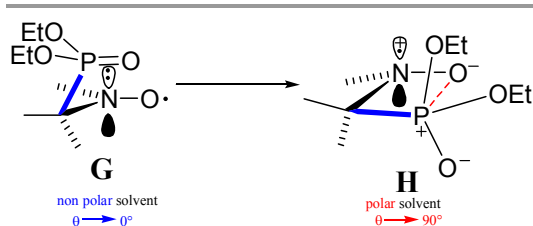
Scheme 7. Conformation change by rotation around the C—N bond from a non polar solvent to a polar solvent

Journal Name

ARTICLE

The choice of the parameters depends on the type of correlation investigated.[##] The Koppel-Palm (eqs. (10) and (11) and the Kalmet – Abboud – Taft (eqs.(15) and (16) relationships are the most popular approaches to describe the solvent effect with specific and non-specific parameters.[13,36,37]

$A = A_0$ + polarity/polarizability terms + hydrogen bonding terms + bulk/cavity terms

(21)

Parameters $f(n^2)$, $f(\varepsilon_r)$, E, B, π^*, E_T^N, α and β are currently applied to describe the solvent effect on physical constants such as spectroscopic data.[13,36,37] The use of the cohesive pressure c, the molar volume V_M and the intrinsic volume V_X is less frequent in such cases.[13] Indeed, the cohesive pressure c is related to the energy required to create cavities in a liquid in order to accommodate solute molecules during the process of dissolution.[13] How this might play a role is not so obvious. In fact, c can also be considered as a parameter describing *the stiffness of structuredness* of the solvent, i.e., the organization of the solvation cage. It is noticed that c increases with the increasing H-bonding capacity of the solvent. The molar volume V_M is often used to take into account the effect of the size of the molecules. However, the weakness of this parameter is that the molecule is described as a sphere.[36] In some cases, this issue is circumvented by using the intrinsic volume V_X as defined by McGowan,[38] which takes partly into account the shape of the molecule, except that it cannot distinguish between isomers. These parameters describing the *structuredness* of the solvent are expected to play a role when a solute exhibits stereocenters and bulky groups.

Multiparameter approach. Analysis of a_N.

As mentioned above, significant scattering was observed for the plots a_N against E_T^N for several nitroxides. Thus, the very popular KP and KAP relationships are applied to get deeper insight into the effects involved in the change in a_N.[13,36,37] All nitroxides are well described by two-parameter KP relationships (Table 5) – E and c for **3•** - **7t•** or $f(\varepsilon_r)$ and c for **3•** - **6c•** and E and $f(n^2)$ for **1•** and **2•**. The use of a bi-parameter equation clearly increases the quality of the correlation (higher R^2 and good F-test, Table 5) and decreases the number of outliers. The absolute values of the parameters provide information on the strength of the effect while the weights (distribution of the effect for each parameter) provide insight into the importance of each effect for each nitroxide. Hence, for **1•** and **2•**, the use of $f(n^2)$ and E is expected from the very good plots reported for a_N vs $E_T(30)$ and eq. (14), as E_T^N is

described as a function of the polarizability $f(n^2)$, the polarity $f(\varepsilon_r)$ and the parameter E.

Interestingly, taking into account the errors, c does not vary significantly with the nitroxide, meaning that the *structuredness* of the solvent in the cybotactic region is the same around the nitroxyl moiety, and its positive value implies that the higher the *structuredness*, the stronger the solvent effect. However, c plays a minor role ($w_c < 40\%$) for **5c,t•** and **7t•** and it has the same weight as E for **4c,t•** and **6t•**. On the other hand, c always plays a major role ($w_c > 60\%$) when $f(\varepsilon_r)$ is the second parameter. In fact, *structuredness* depends a lot on the ability of the solvent to make an H-bond network. Then, as $f(\varepsilon_r)$ describes only the polarity effect of the solvent, the impact of H-bonding in a_N is taken into account by c affording slightly larger values when E is used. Except for **6c•**, the values of E are very close, meaning that the polar and H-bonding properties of the solvent have the same effect on the nitroxyl moieties. This effect is enhanced for **6c•**, likely because the two strong EWGs are close neighbours. This is also observed with the greater influence of E for **6c•** ($w_E = 78$).

When $f(\varepsilon_r)$ is used as parameter, taking into account the errors, all values are in the range $0.6 - 0.7$, except for **6c•** (1.08). As expected, all values are positive. However, their influence is lower ($w_{f(\varepsilon r)} < 35\%$) than the influence of c. Indeed, $f(\varepsilon_r)$ describes only the effect of the polarity of the solvent, implying that the occurrence of H-bonding has a significant influence on the global solvent effect.

However, KP relationships do not seem to be the best approach, as the polar effect of the solvent is either described by the polarity $f(\varepsilon_r)$ or by the Lewis acidity/electrophilic E, and even in two cases by the polarizability.

To circumvent this issue, the KAT relationship (eq. (15)) was applied to **1•** - **7t•**, affording good 3-parameter – π^*, α, and c – correlations, except for **2•** and **3•**. The scattering of the plots E_T^N vs a_N (Figure 9 and Table 2) is significantly decreased, as highlighted by higher R^2 values, good t-test and F-test values (Table 7 and Figure 7SI). Noteworthily, taking into account the errors, all nitroxides experience an effect of the same strength, due to the *structuredness* (cohesive pressure) of the solvent, although its influence (different w_c values) depends strikingly on the structure of the nitroxide. Interestingly, except for **1•** and **6t•**, the influence of α and π^* is evenly shared by all nitroxides whatever the influence of the cohesive pressure. For **1•** and **6t•**, the major effect is the HBD properties of the solvent. As expected from the very good plot E_T^N vs a_N for **1•**, the influence of the cohesive pressure is very weak ($w_c = 12\%$).

For **4•**, **5•**, and **6t•**, the influence of c is roughly the same (w_c ≈35 - 40%), whereas it is significantly lower for **6c•** (w_c = 19%). In fact, **1•** is a highly symmetrical molecule (the four methyl groups are equivalent, due to a fast exchange between the equatorial and axial sites). This implies that the two faces are identical, affording optimal unstrained solvation, and then the *structuredness* of the solvent plays hardly any role. In the case of **2•**, the loss of symmetry (5 methyl groups and a phosphoryl group) is balanced by the free C—N bond rotation, affording an optimized access to the nitroxyl moiety for efficient solvation, and again the *structuredness* of the solvent plays hardly any role. Surprisingly, the loss of symmetry in **3•** is not significant enough to induce a significant effect of the *structuredness* of the solvent. For **4•**, **5•**, **6t•** and **7t•**, the influence of c is moderate, meaning that the substituents around the nitroxyl moiety hamper its solvation, whereas the mobility of the ring combined to the *structuredness* affords a good solvation, hence implying a moderate effect of the *structuredness*. For **6c•**, the repelling effect between the azido group and the phosphoryl group in *cis* relationship is so strong that only one conformation provides the best minimization of the repelling effect, allowing the solvent access to the nitroxyl moiety, and hence leading to a weak influence of the *structuredness* of the solvent. In our case, the effect of parameters π^* and α affords very similar results, i.e., the stabilization of the zwiterionic form **B**, and the discussion will only be provided for α, except for a few cases. The highest HBD effects are reported for **1•** and **2•** (larger w_α). For **4•**, **5•**, **6•** and **7t•**, the same HBD effect is observed. The HBD effect involves a hydrogen bond between the protic solvent and the nitroxyl moiety, and as a consequence, the stronger the interaction, the more favoured form **B**, the higher a_N.

The polarity/polarizability and hydrogen bonding effects strongly favour (positive sign for the coefficients) form **B** (N$^{+\bullet}$—O$^-$ moiety), leading to an increase in a_N with increasing solvent properties. These effects are strengthened by the cohesive pressure c (positive sign for the coefficient) which is used to describe the *structuredness* of the solvent, i.e., higher organization or stronger solvent –solvent intereactions in the cybotactic region will strengthen polarity/polarizability and H-bonding effects. Consequently, the weight of form **H** will be increased.

Multiparameter approach.

Analysis of $a_{\beta,P}$. As mentioned above, significant scattering was observed for the plots $a_{\beta,P}$ against E_T^N for several nitroxides. Moreover, for **3•** and **7t•**, two correlations $a_{\beta,P}$ vs E_T^N were possible, providing at least 10 solvent were excluded. Then, the very popular KP and KAP relationships were applied to get deeper insight into the effects involved in the change in $a_{\beta,P}$. In contrast to the correlation with a_N, KAT and KP approaches are less general. Indeed, the KAT relationship (eq. (16)) is able to describe the solvent effect for **2•** - **7t•**, although this cannot be done with the same set of parameters.

Surprisingly, KP relationships cannot describe the solvent effect for **2•**, whatever the combination of parameters. Except for **3•**, for which only $f(\varepsilon_r)$ and V_M are required, the solvent effect is described by KP relationships using $f(\varepsilon_r)$ and c (see Table 3SI), and the correlations are significantly improved when the size of the solvent molecule V_M is included. However, for the *trans* series, except for **7t•**, the cohesive pressure c can be replaced by the parameter E (see Table 3SI). Consequently, E and c likely describe the same effect: the ability of the first layer of the solvent molecules to develop stabilizing H-bonds with the nitroxyl moiety.

Interestingly, coefficients of $f(\varepsilon_r)$, E, and c are negative, implying that $a_{\beta,P}$ values decrease with increasing properties. In fact, increasing $f(\varepsilon_r)$, E, and c leads to favour the zwiterionic forms of the N—O• (form **B**) and P=O (form **F**) moieties., and, to favour the interaction between N$^{+\bullet}$–O$^-$••••P$^+$–O$^-$ moieties (form **H**) as described in Scheme 7, which, in turn, involved an increase in the dihedral angle θ affording a decrease in $a_{\beta,P}$.

On the other hand, the coefficient of the size of the solvent molecule V_M is positive, meaning that $a_{\beta,P}$ increase with the size of the solvent molecule. That is, the bulkier the solvent is, more hampered the PC—N bond rotation is, and the less favoured form **H** is. Taking into account the errors, the impact of V_M is the same for all nitroxides and its influence is minor (w_{VM} < 25%) on the whole solvent effect. Taking into account the errors, except for **6t•**, the impacts of $f(\varepsilon_r)$ and c are the same for **4•** - **6c•** and their influence is moderate (33% < w_c and $w_{f(\varepsilon r)}$ < 44%) on the global solvent effect. Similar comments hold for the relationships involving $f(\varepsilon_r)$ and E. Interestingly, **6t•**, which carries two strong EWGs in *trans* relationship, exhibits the largest and the smallest coefficients for $f(\varepsilon_r)$ and c, respectively, implying a major influence of $f(\varepsilon_r)$ ($w_{f(\varepsilon r)}$ = 56%) over c (w_c = 19%) and V_M (w_{VM} = 25%).

Unlike the KP relationship, KAT relationships are able to describe the solvent effect on $a_{\beta,P}$ for all nitroxides although this approach is marred by the number of outliers, i.e., 6-10 for **3•**, 5 for **5c•**, 3 for **6t•**, and 7 for **7t•**. Except for **7t•**, for which parameters π^* and V_X are used, the solvent effect for all other nitroxides is described using π^* and α as parameters and the correlations are significantly improved – either better statistical outputs or fewer outliers – by including the size and the shape of the solvent molecule V_X as third parameter. Interestingly, the coefficients of π^* and α are negative, meaning that $a_{\beta,P}$ decrease with increasing polarity/polarizability and the H-bond donor properties of the solvent whereas the positive coefficient for V_X means that $a_{\beta,P}$ increase with the bulkiness of the solvent molecule. This is in nice agreement with the observation made using KP relationships and the comments reported above hold.

Taking into account the errors, the impact of V_X is rougly the same for **4•-6•** and its influence is minor (w_{VX} < 25%) on the global solvent effect. Taking into account the errors, the impact of π^* has a major influence (w_{π^*} > 57%) for **4•-7t•**.

Taking into account the errors, the impact of α is roughly ($w_\alpha \approx$ 17% ± 6) the same for **4•**, **5•**, and **6t•**, slightly lower for **6c** and its influence is very similar to that V_X.

As mentioned above, the solvent effect in **2•** and **3•** is nicely described using π^* and α. As expected, their coefficients are negative. The impact of π^* and α on $a_{\beta,P}$ is clearly stronger in **2•** than in **3•**, in nice agreement with E_T^N trends. However, the weight influence of each parameter is sharply contrasted, that is, the HBD property α is the major effect (w_α = 66%) in **2•** whereas the effect of π^* is the major one (w_{π^*} = 81%) in **3•**. Thus, it seems that less restricted rotations and likely less restricted C—N bond rotations, provided conformations favouring the occurrence of H-bonds in **2•** at the difference of the 5-membered ring nitroxide **3•** in which bond rotations are dramatically restricted. The coefficients obtained for π^* and α given by bi-parametric correlations for **4•-6•** are very similar to those for **3•**, meaning that the same effects are involved to a very close extent. Although different parameters are used for **7t•**, coefficient of π^* and V_X are very similar to those of **3•** given by eq. (16r), meaning that the same effects are again involved.

It stems from the comparing of KAT and KP relationships that the polarity (π^* and $f(\varepsilon_r)$) and the size of the solvent molecules (V_X and V_M) are the main effects, which are antagonist effects, ruling the change in $a_{\beta,P}$. The effect of α and of c is less obvious, as it does not apply to all nitroxides in the same series. Nevertheless, it seems strongly linked to the *stiffness* of the *structuredness* of the solvation cage around the nitroxyl moiety and maybe also around the phosphoryl group.

Although it has a negative coefficient, the polarity/polarizability effect plays a role that is the same for $a_{\beta,P}$ as for a_N, that is, increasing solvent polarity favours both form **B** and form **F**, implying stronger $N^{+\bullet}\!\!-\!O^- \rightarrow P^+\!\!-\!O^-$ interaction and, hence, a more stabilized form **H**. Amazingly, α and c do not apply to all nitroxides and can sometimes be interchanged, meaning that they do not describe their conventional effects. They both probably describe the organization of the solvent molecules around the N—O• and P=O moieties in the cybotactic region, meaning that the higher the *structuredness* (negative coefficients), the stronger the $N^{+\bullet}\!\!-\!O^- \rightarrow P^+\!\!-\!O^-$ interaction. On the other hand, as **4•** - **6•** exhibit strong asymmetry around the nitroxyl moiety, the size of the solvent (V_M of V_X) plays an antagonist role (positive coefficient) to the polarity effect and the *structuredness* of the solvent.

Conclusions

This survey of the solvent effect on new β-phosphorylated nitroxides **3•** - **7t•** unveils an unexpected entanglement of effects, different for a_N and $a_{\beta,P}$, due to the various properties of the solvents. For all nitroxides, a_N values are affected by the polarity/polarizability (π^*), H-bonding (α), and *stiffness* of the *structuredness* (cohesive pressure c) of the solvents. On the other hand, the impact and the occurrence of each effect are less obvious for $a_{P,\beta}$ than for a_N. For example, for **2•** and **3•**, only π^* and α are observed whereas for the cyclic nitroxides π^*, α, c, V_M and V_X are observed. The positive signs for π^*, α, and c mean that a_N values increase with these solvent properties. On the other hand, the negative values for π^*, α and c mean that $a_{\beta,P}$ values decrease with these solvent properties, whereas an antagonist effect is observed with V_X. The anti-correlation between $a_{\beta,P}$ and a_N is ascribed to the $N^{+\bullet}\!\!-\!O^- \rightarrow P^+\!\!-\!O^-$ interaction whose the maximization is the *driving force* of the system. As nitroxides **3•** - **7t•** exhibit changes in $a_{P\beta}$ with the solvent, one possible application of this observation will be the titration of water in organic solvents.

Experimental section

All solvents and reactants were purchased from Aldrich and used as received. Nitroxides **3•**,[20] and **6c•,t•**[35] and **7t•**[35] were prepared according to the literature. Nitroxides **4c•,t•**, and **5c•,t•**, were prepared according to Scheme 1- 4.

Samples were prepared at 0.5 mM nitroxide concentration in non-degassed solvents. Experiments were performed indifferently on Elexsys, EMX or ER 100D Bruker machines (a difference smaller than 0.1 G was noticed). EPR spectra were recorded, the parameters being a gain of 2×10^5 (72 dB for Elexsys), a modulation amplitude of 1.0 G, a sweep width of 150 G, a sweep time of 21 s, and a power of 20 mW.

Acknowledgements

Notes and references

As far as we know this nitroxide has only been observed through spin-trapping experiments involving the addition of 2-diethoxyphoshorylprop-2-yl radical onto *tert*-butyl nitroso. Consequently, its preparation on a large scale is expected to be a challenge by conventional procedures.

§ In general, B_0 is very small and can be neglected. See ref. 10.

† Values of B_1 are dependent on the atom or on the function at position β. See refs. 21 and 10.

‡ In Figure 3, for (a), selective irradiation of these CH_2 signals gave rise to informative NOE cross-peaks (evidenced by green and red boxes) which are due to CH_3 groups as illustrated in (b). This confirmed the *trans* configuration of the 5-membered ring. In contrast, irradiation of the same CH_2 protons in (c) afforded only rise to one NOE cross-peak with the neighboring CH_3 group, in agreement with the expected *cis* configuration.

£ CCDC: 985888.

♫ All figures were very similar.

♪ Other plots are similar.

♠ The Hydrogen Bonding Acceptor HBA property β was not considered, as the investigated nitroxides did not exhibit *"acidic"* proton.

♣ These two relationships are often used to investigate the solvent effects. See ref. 13.

◊ $a_{\beta,P}$ of **4t•**, **5t•** and **6t•** are also described by another 3-parameter KP relationship relying on the polarity $f(\varepsilon_r)$, the acidity/electrophiliy E, and the molar volume V_M, with good statistical outputs (See Table 3SI). Good statistical outputs are obtained when $f(\varepsilon_r)$ and E are used but the scattering decreases when V_M is included (Figure 4SI).

♥ However, for **4c•** and **6c•**, the HBD α parameter might be replaced by c, affording better correlations are observed (see Table 5SI), e.g., for **6c•** (Figure 5SI). For **4c•** and **6c•**, good correlations are observed using π^*, c, and V_X as parameters (Figure 5SI)

♦ Janzen and coll. in ref. 15 reported the same solvent effect (only benzene, methanol, and water have been investigated) for some β-phosphorylated nitroxides. They tentatively ascribed this effect to a change in conformation due to a difference in polarity of the mesomeric forms. Nevertheless, their discussion is very ambiguous and their schemes not convincing, although they might agree with our proposal

Many other parameters available in the literature can be used to describe the different terms of eq. 21. Here, only the parameters used for the KP and KAT correlations are discussed.

1   G. Likhtenshtein, J. Yamauchi, S. Nakatsuji, A. I. Smirnov, R.Tamura, Nitroxides: Applications in Chemistry, Biomedicine, and Materials Science, Wiley-VCH, 2008, and references therein.

2   Stable Radicals: Fundamentals and Applied Aspects of Odd-Electron Compounds (Ed.: R. Hicks), Wiley, Hoboken, 2010, pp. 173–229, and references therein.

3   I. A. Kirilyuk, A. A. Bobko, V. V. Khramtsov, I. A. Grigor'ev, *Org. Biomol. Chem.*, 2005, **3**, 1269–1274.

4   V. Belle, S. Rouger, S. Costanzo, A. Longhi, A. Fournel, Assessing Structures and Conformations of Intrinsically Disordered Proteins (Ed.: V.N. Uversky), Wiley, Hoboken, 2009, and references cited therein.

5   P. Mellet, P. Massot, G. Madelin, S. R. A. Marque, E. Harte, J.-M. Franconi, E. Thiaudière, *PLoS One*, 2009, **4**, e5244.

6   P. Massot, E. Parzy, L. Pourtau, P. Mellet, S. Marque, J.-M. Franconi, E. Thiaudière, *Contrast Media Mol. Imaging*, 2012, **7**, 45–50.

7   H. Karoui, F. Le Moigne, O. Ouari, P. Tordo, *Stable Radicals: Fundamentals and Applied Aspects of Odd-Electron Compounds*, ed. R. Hicks, John Wiley & Sons, 2010, pp. 173–229.

8   V. Ovcharenko, *Stable Radicals: Fundamentals and Applied Aspects of Odd-Electron Compounds*, ed. R. Hicks, John Wiley & Sons, 2010, pp. 461–506.

9   B. Knauer, J. J. Napier, *J. Am. Chem. Soc.,* 1976, **98**, 4395 – 4400.

10   E. G. Janzen, G. A. Coulter, U. M. Oehler, J. P. Bergsma, *Can. J. Chem.*, 1982, **60**, 2725–2733.

11   C.-H. Deng, C.-J. Guan, M.-H. Shen, C.-X. Zhao, *J. Fluorine Chem.*, 2002, **116**, 109–115.

12   A. Sh. Mukhtarov, A. V. Il'Yasov, Ya. A. Levin, I. P. Gozman, M. S. Skorobogatova, E. I. Zoroatskaya, *Theor. Exp. Chem.* **1976**, *12*, 656–660; *Teor. Eksp. Khim.,* 1976, **12**, 831 – 836.

13   C. Reichardt, T. Welton, Solvent and Solvent Effect in Organic Chemistry, 4th ed., Wiley-VCH, Weinheim, **2011**.

14   C. Reichardt, *Chem. Rev.*, 1994, **94**, 2319-2358.

15   D. L. Haire, E. G. Janzen, G. Chen, V. J. Robinson, I. Hrvoic, *Magn. Reson. Chem.,* 1999, **37**, 251-258.

16   S. Marque, C. Le Mercier, P. Tordo, H. Fischer, *Macromolecules*, 2000, **33**, 12, 4403-4410.

17   G. Audran, L. Bosco, P. Brémond, T. Butscher, S. R. A. Marque, G. Obame, *Appl. Magn. Reson.*, 2015, *in press* DOI 10.1007/s00723-015-0649-4.

18   G. Audran, L. Bosco, P. Brémond, T. Butscher, S. R. A. Marque *Chem. Commun*, *submitted.*

19   G. Audran, L. Bosco, P. Brémond, T. Butscher, J.-M. Franconi, S. R. A. Marque, P. Mellet, E. Parzy, M. Santelli, E. Thiaudière, *Org. Biomol. Chem.,* 2015, ASAP

20   F. Le Moigne, A. Mercier, P. Tordo, *Tetrahedron Lett.*, 1991, **32**, 3841-3844.

21   F. Gerson, W. Huber, Electron Spin Resonance Spectroscopy of Organic Radicals, Wiley-VCH, Weinheim, 2003.

22   S. Acerbis, D. Bertin, B. Boutevin, D. Gigmes, P. Lacroix-Desmazes, C. Le Mercier, J.-F. Lutz, S. R. A. Marque, D. Siri, P. Tordo, *Helv. Chim. Acta*, 2006, **89**, 10, 2119-2132.

23   C. Mathieu, A. Mercier, D. Witt, L. Dembkowski, P. Tordo, *Free Rad. Biol. Med.*, 1997, **22**, 802-806.

24   C. Ricci, S. Marque, F. Belin, J.-C. Bouteiller, R. Lauricella, B. Tuccio, V. Cerri, P. Tordo *J. Chem. Soc., Perkin Trans. 2*, 1997, 2513-2518.

25   A. Alberti, Nitroxides radicals and polynitroxides in Landolt-Börnstein, New Series II/26D, Ed. H. Fischer, Springer-Verlag, Heidelberg, 2005, 7-537 and references therein.

26   J.-L. Clément, B. C. Gilbert, W. F. Ho, D. N. Jackson, M. S. Newton, S. Silvester, G. S. Timmins, P. Tordo, A. C. Whitwood, *J. Chem. Soc. Perkin Trans. 2*, 1998, 1715-1717.

27   F. Fréjaville, H. Karoui, B. Tuccio, F. Le Moigne, M. Culcasi, S. Pietri, R. Lauricella, P. Tordo, *J. Med. Chem.*, 1995, **38**, 258-265.

28   P. Stipa, J.-P. Finet, F. Le Moigne, P. Tordo, *J. Org. Chem.*, 1993, **58**, 4465-4468.

29   L. Dembkowski, J.-P. Finet, C. Fréjaville, F. Le Moigne, R. Maurin, A. Mercier, P. Pages, P. Stipa, P. Tordo, *Free Rad. Res. Comms.*, 1993, 19, S23-S32.

30   Gigmes, D.; Marque, S. R. A. *"Nitroxide Mediated Polymerization and its Applications"* Encyclopedia of Radicals in Chemistry, Biology, and Materials Chatgilialoglu, C., Studer, A., Eds.; Wiley: Chichester, U.K., 2012, 1813-1850.

31   D. Bertin, D. Gigmes, S. R. A. Marque, P. Tordo, *Chem. Soc. Rev.,* 2011, **40**, 2189-2198.

32   E. G. Bagryanskaya, E. G. Krumkacheva, M. V. Fedin, S. R. A. Marque, *Methods Enzym.,* 2015, **563**, 365-396.

33   G. Audran, L. Bosco, P. Brémond, J.-M. Franconi, N. Koonjoo, S. R. A. Marque, P. Massot, P. Mellet, E. Parzy, E. Thiaudière, *Angew. Chem. Int. Ed.* 2015, **54**, 45, 13379-13384.

34   D. Benoit, V. Chaplinski, R. Braslau,; C. J. Hawker, *J. Am. Chem. Soc.*, 1999, **121**, 3904–3920.

35   N. Le Breton, M. Martinho, K. Kabitaev, J. Topin, E. Mileo, D. Blocquel, J. Habchi, S. Longhi, A. Rockenbauer, J. Golebiowski, B. Guigliarelli, S. R. A. Marque, V. Belle, *PhysChemChemPhys*, 2014, **16**, 4202-4209.

36   Y. Marcus, *The Properties of Solvents*, Vol. 4, Wiley, Chichester, 1998.

37   G. E. Zaikov, R. G. Makitra, G. G. Midyana, L. I. Bazylyak, *Influence of the Solvent on Some Radical Reaction* Chemistry Research and Applications Series, Nova Science Publishers Inc., New York, 2010.

38   J. C. McGowan, *J. Appl. Chem. Biotechnol.*, 1978, **28**, 599.

39   D. Bertin, D. Gigmes, S. R. A. Marque, P. Tordo, *Macromolecules*, 2005, **38**, 7, 2638-2650.

40   J. Shorter, Correlation Analysis of Organic Reactivity; J. Wiley & Sons: New York, 1982, 73-126.

41   J. B. Sweeney, *Chem. Soc. Rev.*, 2002, **31**, 247-258.

42   M. Charton, *Prog. Phys. Org. Chem.*, 1981, **13**, 119-251.

43   A. R. Katritzky, D. C. Fara, H. F. Yang, K. Tamm, T. Tamm, M. Karelson, *Chem. Rev.*, 2004, **104**, 175-198.

44 I. A. Koppel, V. A. Palm, The Influence of the Solvent on Organic Reactivity, in N. B. Chapman and J. Shorter (Eds.): Advances in Linear Free Energy Relationships, Plenum Press, London, New York, 1972, Chapter 5, p. 203¤.

a_N and a_P of β-phosphotylated 5-memebered ring nitroxides are sensitive to the polarity/polarisability π*, the strucduredness of the solvent c, and to the Hydrogen Bond Donating α properties of the solvent.

a_N and a_P of β-phosphotylated 5-memebered ring nitroxides are sensitive to the polarity/polarisability π*, the strucduredness of the solvent c, and to the Hydrogen Bond Donating α properties of the solvent.